(3)

THE OHIO STATE UNIVERSITY

JOINT SERVICES ELECTRONICS PROGRAM

Eleventh Annual Report

The Ohio State University

ElectroScience Laboratory

Department of Electrical Engineering
Columbus, Ohio 43212

Annual Report 720440-1
Contract No. N00014-88-K-0004
November 1988

Department of the Navy
Office of Naval Research
800 North Quincy Street
Arlington, Virginia 22217

NOTICES

When Government drawings, specifications, or other data are used for any purpose other than in connection with a definitely related Government procurement operation, the United States Government thereby incurs no responsibility nor any obligation whatsoever, and the fact that the Government may have formulated, furnished, or in any way supplied the said drawings, specifications, or other data, is not to be regarded by implication or otherwise as in any manner licensing the holder or any other person or corporation, or conveying any rights or permission to manufacture, use, or sell any patented invention that may in any way be related thereto.

ADA204819

50272-101

REPORT DOCUMENTATION PAGE	1. REPORT NO.	2.	3. Recipient's Accession No.
4. Title and Subtitle JOINT SERVICES ELECTRONICS PROGRAM Eleventh Annual Report			5. Report Date November 1988 6.
7. Author(s) Leon Peters, Jr.			8. Performing Organization Rept. No. 720440-1
9. Performing Organization Name and Address The Ohio State University ElectroScience Laboratory 1320 Kinnear Road Columbus, Ohio 43212			10. Project/Task/Work Unit No. 11. Contract(C) or Grant(G) No (C) N00014-88-K-0004 (G)
12. Sponsoring Organization Name and Address Department of the Navy Office of Naval Research 800 North Quincy Street Arlington, VA 22217			13. Type of Report & Period Covered Annual Report 10/1/87 - 9/30/88 14.

15. Supplementary Notes

16. Abstract (Limit: 200 words)

17. Document Analysis a. Descriptors

b. Identifiers/Open-Ended Terms

c. COSATI Field/Group

18. Availability Statement	19. Security Class (This Report)	21. No of Pages
Approved for Public Release: Distribution is Unlimited	Unclassified	84
	20. Security Class (This Page) Unclassified	22. Price

(See ANSI-Z39.18) See Instructions on Reverse

OPTIONAL FORM 272 (4-77)
(Formerly NTIS-35)
Department of Commerce

Contents

List of Figures

I. DIRECTORS OVERVIEW

This report represents the eleventh annual summary of The Ohio State University Joint Services Program (JSEP).

There have been a total 23 Ph.D. and 16 M.Sc degrees in Electrical Engineering obtained under partial JSEP sponsorship. There are currently 6 Ph.D. and 2 M.Sc. students being partially supported under JSEP.

As may be seen in the Annual report Appendix, 15 reprints have been included in the period September 1987 to September 1988. In addition, 20 papers have already been accepted for publication in the coming year, an additional 12 papers have been submitted, and an additional 9 papers are in preparation.

II. DESCRIPTION OF SPECIAL ACCOMPLISHMENTS AND TECHNOLOGY TRANSITION

The transfer of the compact range and target identification technology initiated under JSEP support for time domain studies continues to make large advances. A new and yet improved design for the compact reflector has now been generated.

The research has proven to be of intense interest to DOD. and the Aerospace industry and we have now added three new members to our Compact Range Consortium. There are now 13 members. The new members are Mission Research and Loral and Norden. These 13 members represent a major cross section of the Aerospace and Electronic Industries. This activity will continue to grow and is all being achieved with external support including additional major support from several DOD agencies. In fact this total support in these experimental studies substantially now exceeds our

JSEP support. Agencies This research is truly guiding a major portion of this technology in the USA and is extremely important for stealth technology advances. However, these advances were only possible because of the initial JSEP support. This is certainly a case where a small investment of basic research funds have been leveraged to generate much larger support.

Our target identification work also partially funded at one time under JSEP Time Domain Studies is also being funded by several other agencies including ONR and continues to be rather vigorous. Again, JSEP funds have been leveraged to initiate larger programs.

Our JSEP research continues to focus on Electromagnetic related topics. There are three major electromagnetics areas that were pursued in the past year and a closely related study in Adaptive Arrays.

The goal of our Diffraction Studies is to not only treat new diffracting mechanisms but also to reduce their complexity so that they can be more readily applied to DOD problems. These mechanisms become exceedingly important as stealth technology advances, i.e., as scattered fields are reduced ever lower. It is the intent to reduce these analyses to the Diffraction Coefficient format so that the solution of scattered/radiated fields for aerospace vehicles will involve the use of these coefficients and differential geometry. Such solutions will then be packaged in a variety of computer codes on other projects as part of a technology transfer mechanism.

Our Integral Equation Studies have focussed attention on the analysis of penetrable materials used in conjunction with conducting surfaces. These have included various tactics to reduce the computation time required such as making use of special Green's functions so that only the unknowns are currents in the materials. Future research in this area will involve much more general media so that we are now introducing and treating chiral and

non-linear media via the integral equations approach.

The Hybrid Approach represents novel analyses involving more than one basic technique such as was done originally at the ESL by combining diffraction and integral equations which was one of the earlier such solutions. One of our initial efforts involved the scattering from structures that resembled jet intakes and exhausts. Several decades ago, these were supposedly geometries whose scattering properties would never be treated analytically with any degree of success. Our recent work has been overcoming most of these difficulties as will be seen in the deep cavities discussed in the appropriate section. Both government and industry are becoming the primary supporters for this effort and again JSEP support has been used in the initial stages of study that have been carried to the extent that others are now providing the major funding. Research on more shallow antenna cavities is also continuing and we expect that this effort will also be of general interest to many.

Another topic of interest here is the electromagnetic properties of stripline systems. To treat such devices rigorously requires the inclusion of a very complex Sommerfeld integral. Asymptotic forms of this integral have been obtained that greatly simplifies such analyses.

An adaptive array study provided new results on how such arrays affect bit error probabilities when used in BPSK, DPSK, QPSK, and FSK communication systems subjected to CW and broadband jamming signals. Previous research on adaptive arrays has characterized array performance in terms of output signal-to-interference-plus-noise ratio (SINR). While SINR is one measure of performance, it does not provide a complete picture of the array performance because it does not take signal and jammer waveforms into account. The results of this work were published in a series of three

papers.

Finally, under JSEP we have explored the novel idea of using adaptive arrays in packet radio systems. We have shown that an adaptive antenna used in a packet repeater results in a substantial increase in system throughput. It does this by preventing packets that arrive at nearly the same time from colliding, while also protecting the repeater from jamming and spoofing. When adaptive arrays are used in packet radio networks, routing and stability problems in these networks can be substantially reduced. We believe that this technique, which is not yet being considered by the packet radio community, could substantially improve packet network performance.

Technology transition continues to take several forms for our JSEP program. First, of course, are the students graduating in this program who carry the knowledge gleaned in their research programs to other users. Second, there are the published papers, both oral and written, which generally attract the attention of other DOD sponsoring agencies. Such agencies in turn provide additional funding and in general make use of our JSEP research and to extend it to better their own programs.

A fourth method of technology transfer lies in the short course area. Our Uniform Theory of Diffraction has been taught for a number of years and has been attended by members of DOD, industry, universities and also by a variety of foreign scientists and engineers. The fifth method takes the form of computer codes developed under non-JSEP sources that make extensive use of JSEP research. As we have noted previously, the results of all of these studies are of great importance in the analysis and control of the scattering from complex shapes.

This continues to be a major task at The Ohio State University ElectroScience Laboratory (OSU-ESL) which is funded by a variety of DOD

agencies. The ultimate goal is to provide a general computer code (or codes) for the evaluation of the RCS of Aerospace vehicles, but a variety of theoretical analysis must be generated before this goal can become a reality. The OSU-ESL continues to provide a variety of computer codes for radiation from antennas on aircraft, reflector antennas and integral equation formulations based on previous research activities to 62 industrial organizations with DOD approval for use in DOD activities. In fact, last year 114 additional copies of these very complex user friendly codes were issued. Revised versions incorporating newer results are in progress at this time again as funded by other agencies. Three OSU personnel involved in JSEP are members of an advisory committee to assist in plans for a DOD consortium to develop major vehicular scattering codes. JSEP personnel and concepts developed and those currently being pursued with our JSEP support are expected to play a substantive role in these plans.

III. DIFFRACTION STUDIES

Researchers:

R.G. Kouyoumjian, Professor	(Phone: 614/292-7302)
P.H. Pathak, Associate Professor	(Phone: 614/292-6097)
N. Wang, Research Scientist	(Phone: 614/292-0220)
R. Rojas, Senior Research Assoc.	(Phone: 614/292-2530)
R. Tiberio, Visiting Professor	
C.D. Chuang, Research Scientist	(Phone: 614/292-5846)
K.C. Hill, Graduate Research Assoc.	(Phone: 614/294-9283)
M.C. Liang, Graduate Research Assoc.	(Phone: 614/294-9281)
L.M. Chou, Graduate Research Assoc.	(Phone: 614/294-9280)
H.C. Ly, Graduate Research Assoc.	(Phone: 614/294-9281)

1. Introduction

The research in diffraction studies is aimed at primarily developing uniform geometrical theory of diffraction (UTD) analysis of new and important canonical problems which serve to significantly extend the capabilities of ray methods for treating EM radiation and scattering from electrically large complex objects.

During the past period, substantial progress has been made in the development of uniform asymptotic high frequency (or UTD) analysis of the diffraction by both perfectly conducting and non-conducting canonical shapes of importance to present and future EM technology. In particular, the accomplishments are:

i. The development of a generalized UTD analysis for the diffraction by a wedge with convex faces which includes surface ray effects and grazing angles of incidence/diffraction on the convex faces. All previous edge diffraction solutions ignored the latter effects thereby limiting their usefulness

to directions of incidence/diffraction which are far from the convex surface shadow boundaries. The present generalization removes the above deficiencies present in the previous solutions; furthermore, it sheds light on the coupling between edge and surface diffraction phenomena.

ii. The development of UTD analysis for the diffraction by non-conducting surfaces. A key step in the accurate treatment of perfectly-conducting surfaces with a moderately thin layer of material coating has been tied to the generalized impedance boundary conditions developed during the past period. This has been useful for analyzing the diffraction by 2-D and 3-D material half-planes on a ground plane; the diffraction by a material half-plane; the diffraction by a perfectly-conducting half plane which is material coated on both sides, and in which the coting could also be of finite extent. Also, the diffraction by the junction between two thin dissimilar material half planes has been analyzed. The latter analysis together with the related generalized resistive boundary condition also developed in the past period now opens up a wide clan of configurations involving junctions between resistive sheets and between resistive and perfectly conductive sheets, etc. which will be analyzed in the future.

iii. The refinement of previous corner diffraction and edge wave excitation solutions in the search of a more complete treatment for corner and edge wave diffraction mechanisms. This work is still in progress, but the solution based on refinements to this point look encouraging.

The work on the above topics is summarized in somewhat more detail in the following sections.

2. Development of a Generalized UTD Solution for the Diffraction by a Wedge with Convex Faces

A uniform geometrical theory of diffraction (UTD) analysis for an edge in an otherwise smooth perfectly conducting surface developed previously by Kouyoumjian and Pathak [*Proc. IEEE*, pp. 1448-1461, Nov. 1974] has been applied successfully for solving a large variety of antenna/scattering problems of engineering interest. However, that UTD edge diffraction solution fails for directions of incidence and diffraction which are close to grazing on the curved faces of the wedge; it also does not contain information on the surface rays which are launched on the convex faces of the wedge via edge diffraction.

A generalized UTD (GUTD) solution has been developed such that it overcomes the above limitations of the previous UTD edge diffraction solution. This GUTD solution can accurately describe both the rays diffracted by the wedge directly into space as well as the effects of the surface rays excited/diffracted by the wedge when the illumination is due to a source that can be either on or off the convex faces of the wedge. The present UGTD solution is constructed via an asymptotic matching procedure, and it contains more complicated transition functions than those present in the previous UTD edge diffraction solution. These new transition functions allow for the overlap of two or more asymptotic wave transition regions which are adjacent to the incident, reflected, and the various surface shadow boundaries; such an overlap of different transition layers occurs for grazing angles of incidence and/or diffraction. The present UGTD solution recovers, as a special case, the partially generalized UTD edge diffraction solution [Hill

and Pathak, 1987 *URSI Radio Science* Meeting, Virginia, June 15-19] which describes the excitation/diffraction of surface rays as long as one is not close to grazing angles of incidence/diffraction and provided there are no overlapping transition regions. The accuracy of this new GUTD solution has been established by comparison with independent moment method solutions to semi-circular cylinders and ogival shapes. Two papers have been written on this topic; one of these is to appear in Radio Science and the other will be submitted for publication.

3. Diffraction by Non-Conducting Surfaces

The EM scattering from perfect electric conducting objects with thin material coatings is an important area of research. As is well known, the high-frequency EM scattering from complex structures can be synthesized from the solutions of simpler geometries which are referred to as canonical geometries; e.g., half-plane, wedge, circular cylinder, sphere, etc. However, the analysis of these canonical geometries is fairly complicated when they exhibit a thin material coating. Since in scattering problems one is interested in the fields outside the dielectric layers, a key step to simplify the original problem is to replace the coated surfaces by Generalized Impedance Boundary Conditions (GIBC) which have been developed during the past period. The details of how this is accomplished are discussed in two papers by Rojas, one of which has been published and th other is to appear in *Radio Science*. Note that related boundary conditions referred to as the Generalized Resistive Boundary Conditions (GRBC) are also obtained in the latter paper for a planar dielectric (transparent) slab.

The GIBC/BRGC are generalizations of the well known Leontovich/resistive boundary conditions. Thus, if the canonical geometries, which satisfy the usual impedance/resistive boundary condition can be analyzed, they can

also be analyzed when they satisfy the more general GIBC/GRBC. The methods of analysis that one can resort to for planar surfaces characterized by GIBC/GRBC are the Wiener-Hopf and the Generalized Reflection method (Maliuzhnets method).

Several canonical problems have been solved recently using the "GIBC/GRBC procedure". The first one is the diffraction by a thin dielectric half-plane in free space and also backed by a PEC plane. That geometry was also analyzed previously using a less rigorous approximation for the boundary conditions. The present solution provides a further improvement. Another canonical geometry that has been solved recently is the diffraction by a coated PEC half-plane, where the coating is the same on both faces of the half-plane. The coating can also be of finite length, which means that the interactions between the edges of the coating are also taken into account. A related geometry to the coated half-plane configuration is the diffraction by the junction of two, thin dissimilar material half-planes. This canonical problem has also been solved.

4. Analysis of the Phenomena of corner and Edge Wave Diffraction

Progress continues to be made in the analysis of corner and edge wave diffraction phenomena. An analysis has been presently developed for the diffraction of an EM plane wave by a corner (vertex) in a planar conducting surface. This analysis employs an asymptotic approximation for the induced current based on geometrical optics and edge diffracted as well as approximate edge wave fields. These induced currents are used within the radiation integral over the surface of the plane angular sector containing the corner; the latter integral is evaluated in the semi-infinite domain using uniform asymptotics, whereas; it is integrated numerically over the

remaining domain corresponding to the finite angular extent of the corner. At present, refinements to the asymptotic integration over the semi-infinite domain are being studied carefully; also, refinements to the asymptotic approximation for the induced current are being studied simultaneously, as both these refinements are crucial to the accuracy of the corner diffraction and edge wave diffraction solution. While these corner and edge wave phenomena are rather difficult to analyze, a lot more has been learned about them during the past years effort. It is hoped that this would provide steps leading to a more complete treatment in the future.

5. Other Diffraction Mechanisms

A uniform solution valid across smooth caustics of rays reflected by surfaces which are concave or which contain points of inflection has been developed. This solution recovers not only the real geometrical optics ray fields on the lit side of the caustic, but it also recovers the complex geometrical optics ray fields (as postulated by Ikuno and Felsen, *J. Radio Science*, vol. 22, No. 6, pp. 952-958, Nov. 1987) on the dark side of caustics. This solution is of interest in the analysis of the scattering of waves by smoothly indented boundaries. A paper describing this work has been submitted for publication.

6. Creeping Wave Analyses

a. Scattering by a Coated Elliptic Cylinder

During the current reporting period we investigated the scattering by an elliptic cylinder with dielectric material coating. The cross-sectional view of the elliptic cylinder with dielectric coating is illustrated in Figure 1. Note that the thickness of the coating can be uniform or nonuniform. However,

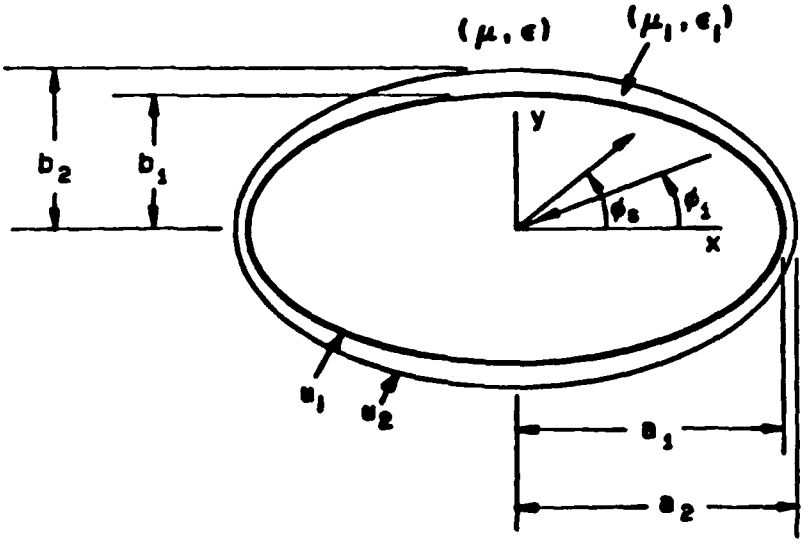

Figure 1: Cross-sectional view of elliptic cylinder with dielectric coating.

eigenfunction solutions exist only for a nonuniform thickness as shown in Figure 1. The dielectric material has a complex permeability μ_r and a permittivity ϵ_r. We have developed a GTD solution for the scattering by the coated elliptic cylinder. The solution consists of the usual geometric-optic terms and the creeping-wave residue series. Based upon the locality of the high frequency solution, we assume that a creeping wave is excited at the grazing point at the dielectric/air interface. It traverses along the interface, and tangentially sheds energy to the scattering direction. It is believed that this is the first available GTD solution for the scattering by the coated elliptic cylinder. Figures 2 to 5 illustrate some preliminary results for the backscatter echo width versus the semimajor axis a_1/λ_o, where λ_o is the free space wavelength. In these figures, the eigenfunction solution obtained by Professor Richmond [1] is plotted in dashed lines, whereas, the solid lines are the GTD results. Some comments are in order. It is noted that for $\phi^i = 90^o$ incidence, the agreement between the eigenfunction results and the GTD results are very good both for the TE and TM cases. However,

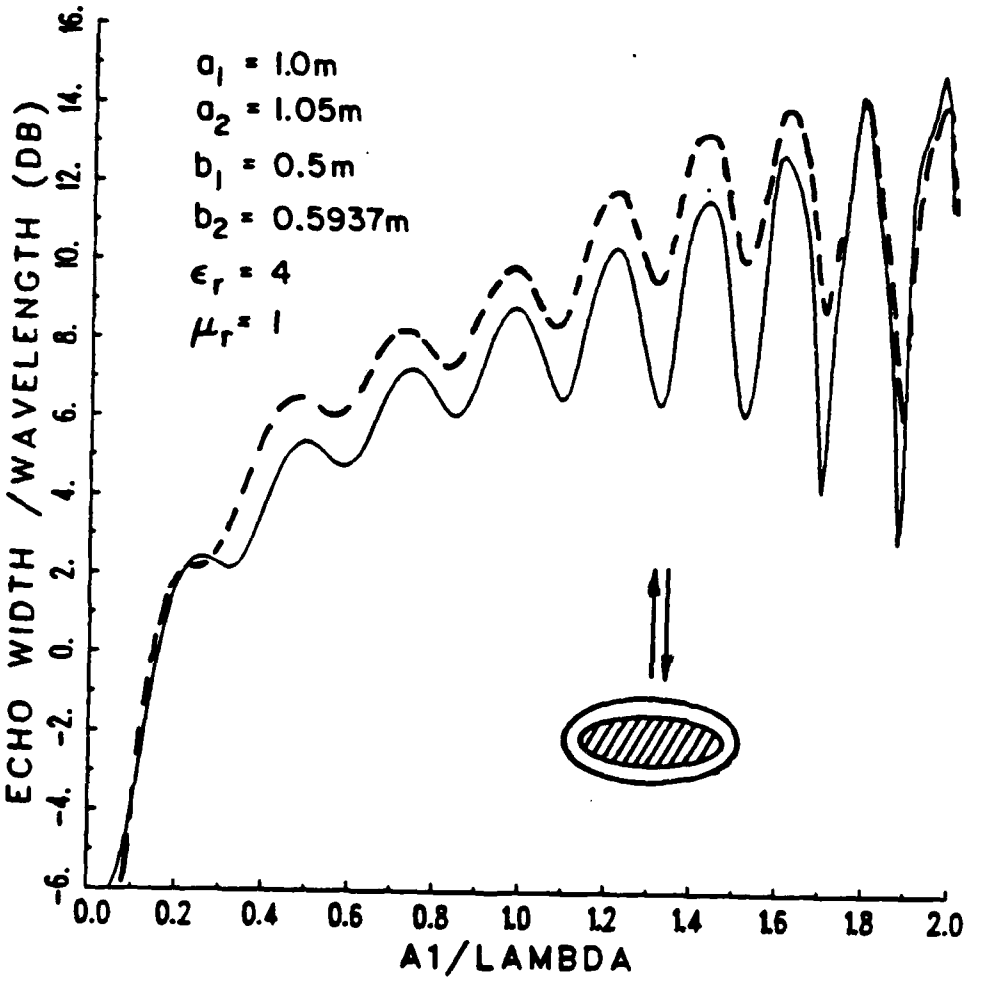

Figure 2: Backscatter for dielectric coated elliptic cylinder with TE polarization, $\phi_i = 90°$.

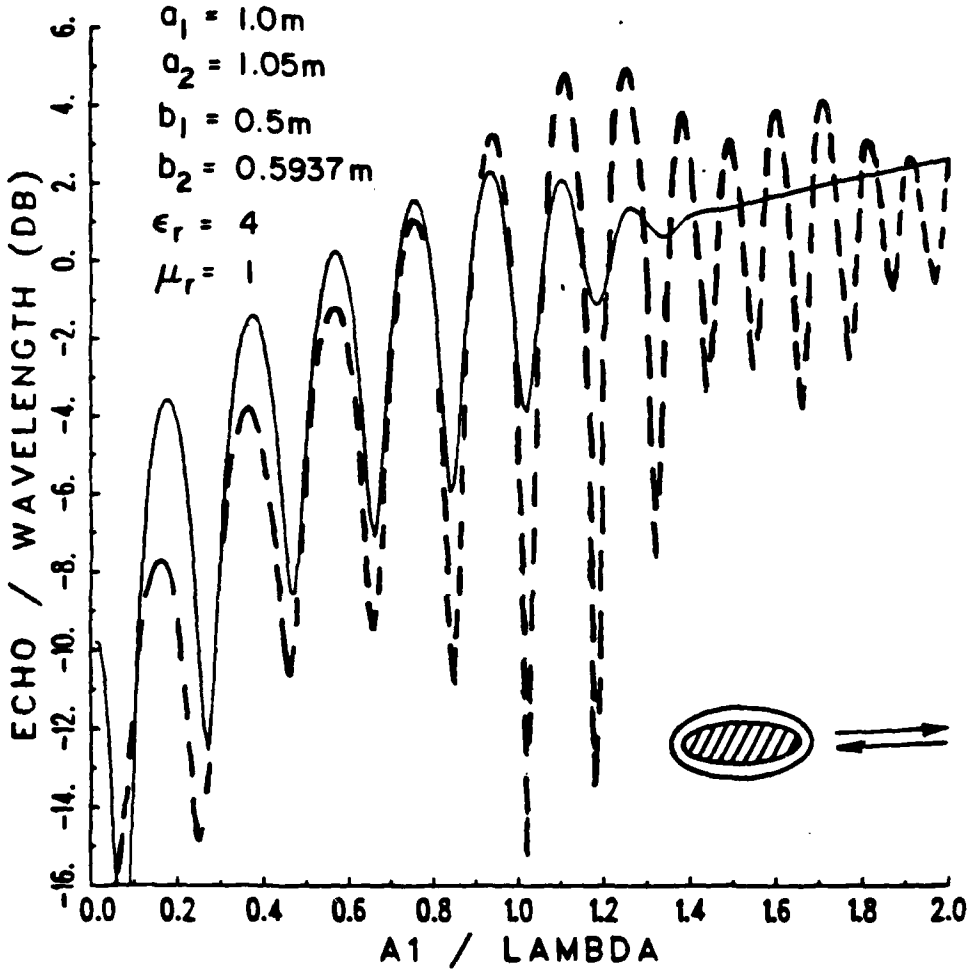

Figure 3: Backscatter for dielectric coated elliptic cylinder with TE polarization, $\phi_i = 0°$.

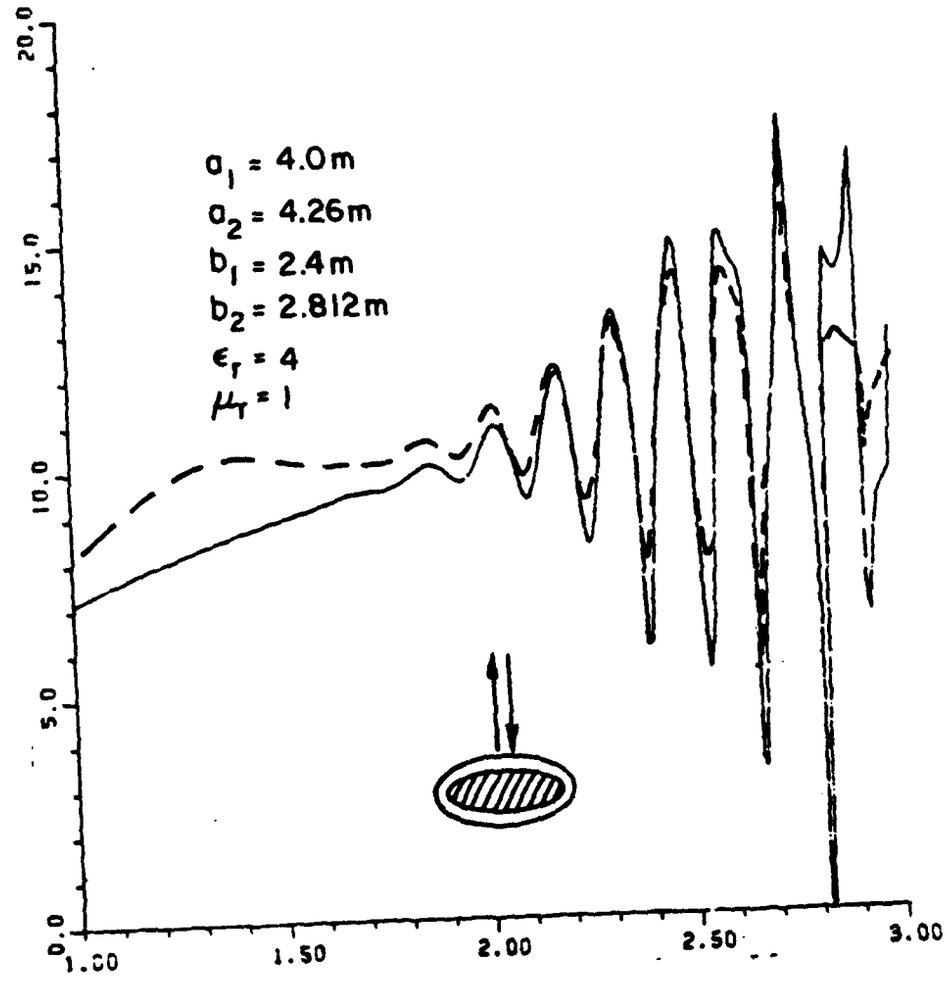

Figure 4: Backscatter for dielectric coated elliptic cylinder with TM polarization, $\phi_i = 90°$.

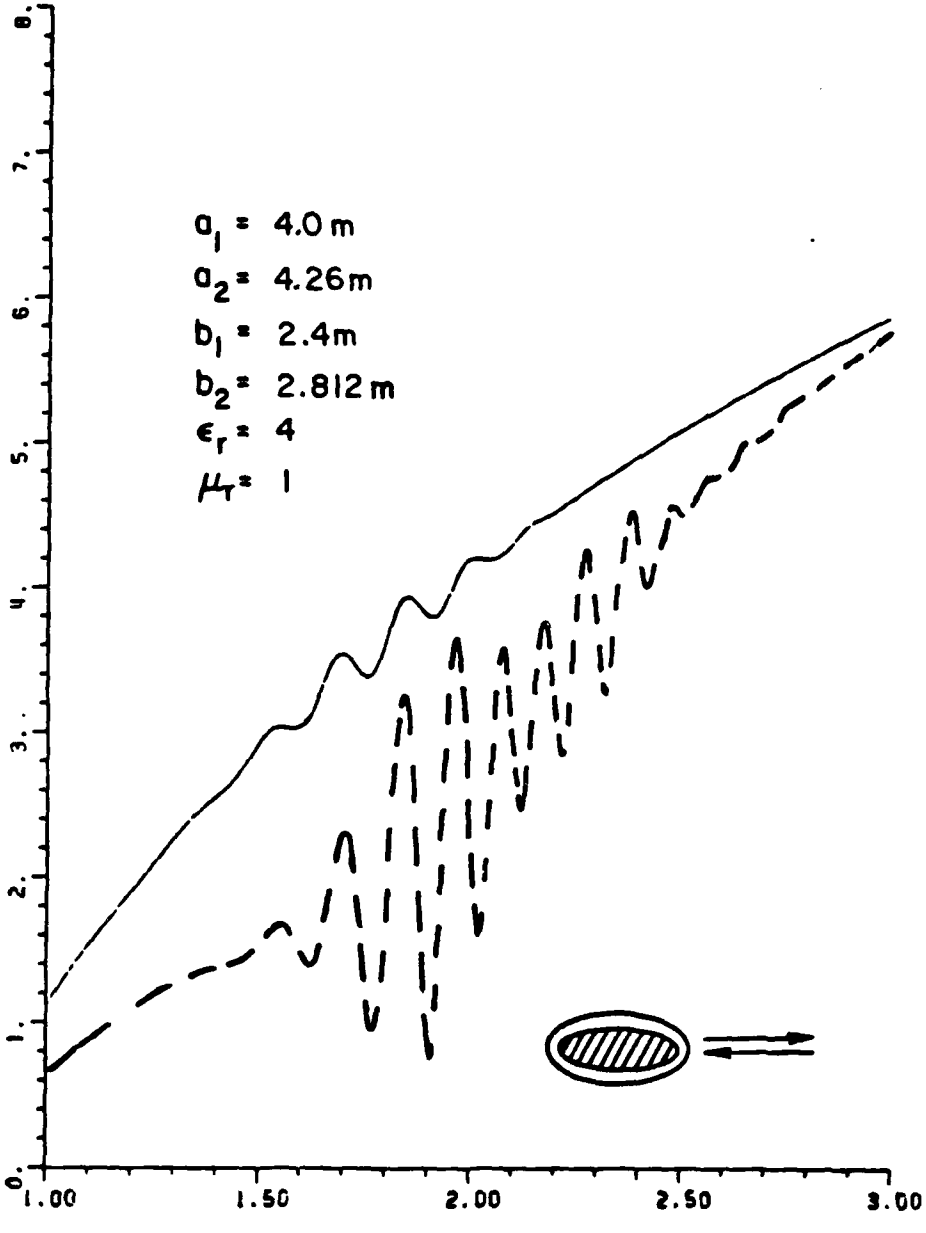

Figure 5: Backscatter for dielectric coated elliptic cylinder with TM polarization, $\phi_i = 0°$.

for the $\phi^i = 0^o$ incidence, the disagreement between them is evident. One possible reason for the discrepancy could be that the nonuniform thickness of the dielectric coating will introduce scattering mechanisms for the $\phi^i = 0^o$ case which are new to the GTD concept. This speculation is very interesting and needs to be further investigated.

In some applications, a uniform coating thickness may be desirable. Figures 6 to Figure 9 present the backscattering echo width for an elliptic cylinder with uniform coating. Only GTD results are shown, since no eigenfunction solution exists for this geometry.

b. Pulse-Galerkin Formulation for the Scattering by a Coated Cylinder

During the current reporting period, we also developed a simple computer code to calculate the radiation and scattering from a coated cylinder with arbitrary cross section. This code will be employed to validate other solutions for the coated cylinder, e.g., the eigenfunction solution and/or the GTD solution. The problem is formulated in terms of coupled boundary integral equations, with equivalent sources for the external and internal regions as unknowns. The field inside the coating can be considered to be produced by the equivalent source g_e on the conducting surface and g_1 on the dielectric/air interface, radiating into unbounded homogeneous space filled with the dielectric of permittivity ϵ_r and permeability μ_r everywhere. Similarly, the scattered field can be considered to be produced by equivalent sources g_o on the dielectric/air interface radiating into unbounded free space. The boundary conditions to be satisfied are the continuity of tangential E and H over the dielectric/air interface and tangential $E = 0$ on the conducting surface. The coupled integral equations are reduced to

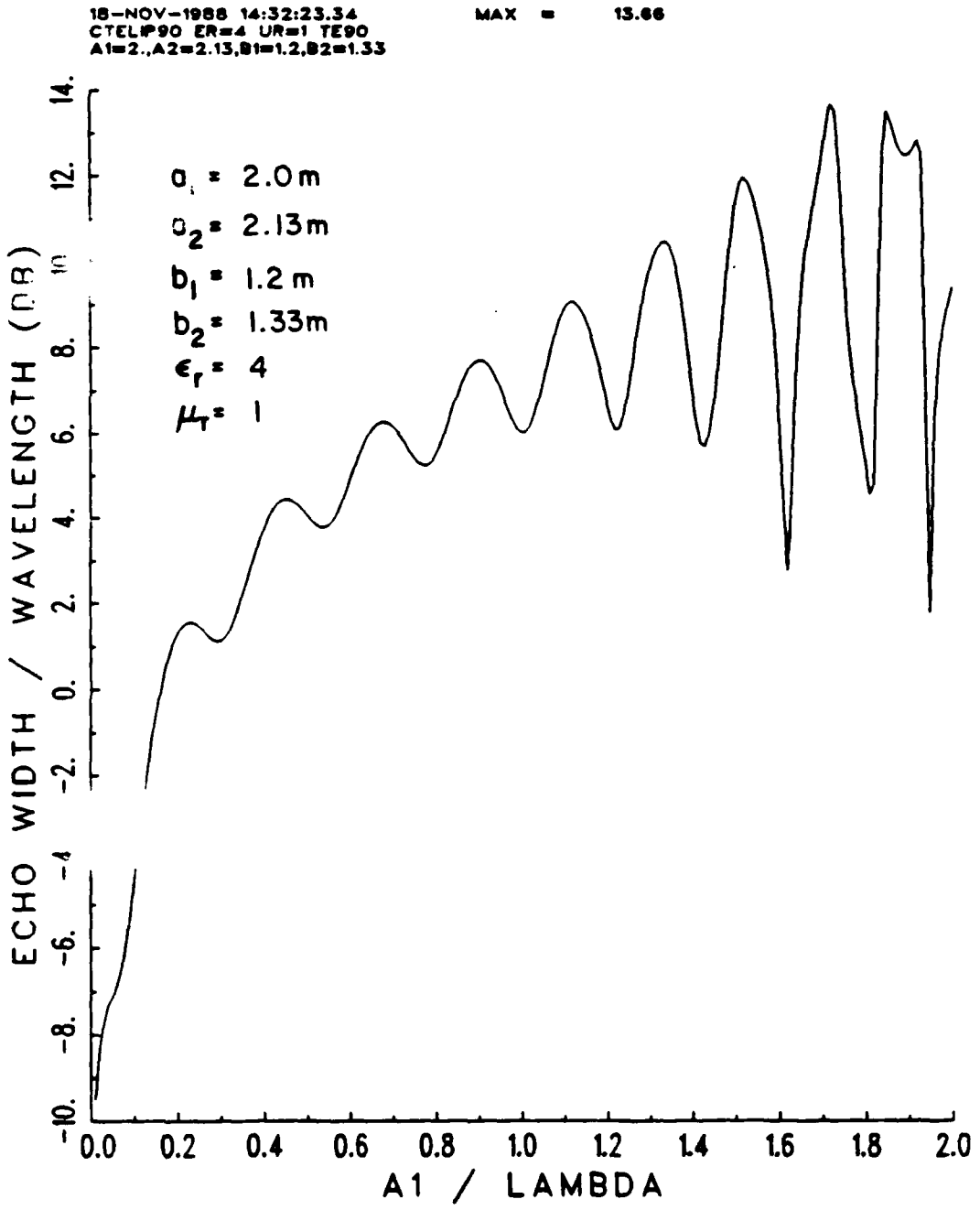

Figure 6: Backscatter for elliptic cylinder with uniform dielectric coating, TE polarization; $\phi_i = 90°$.

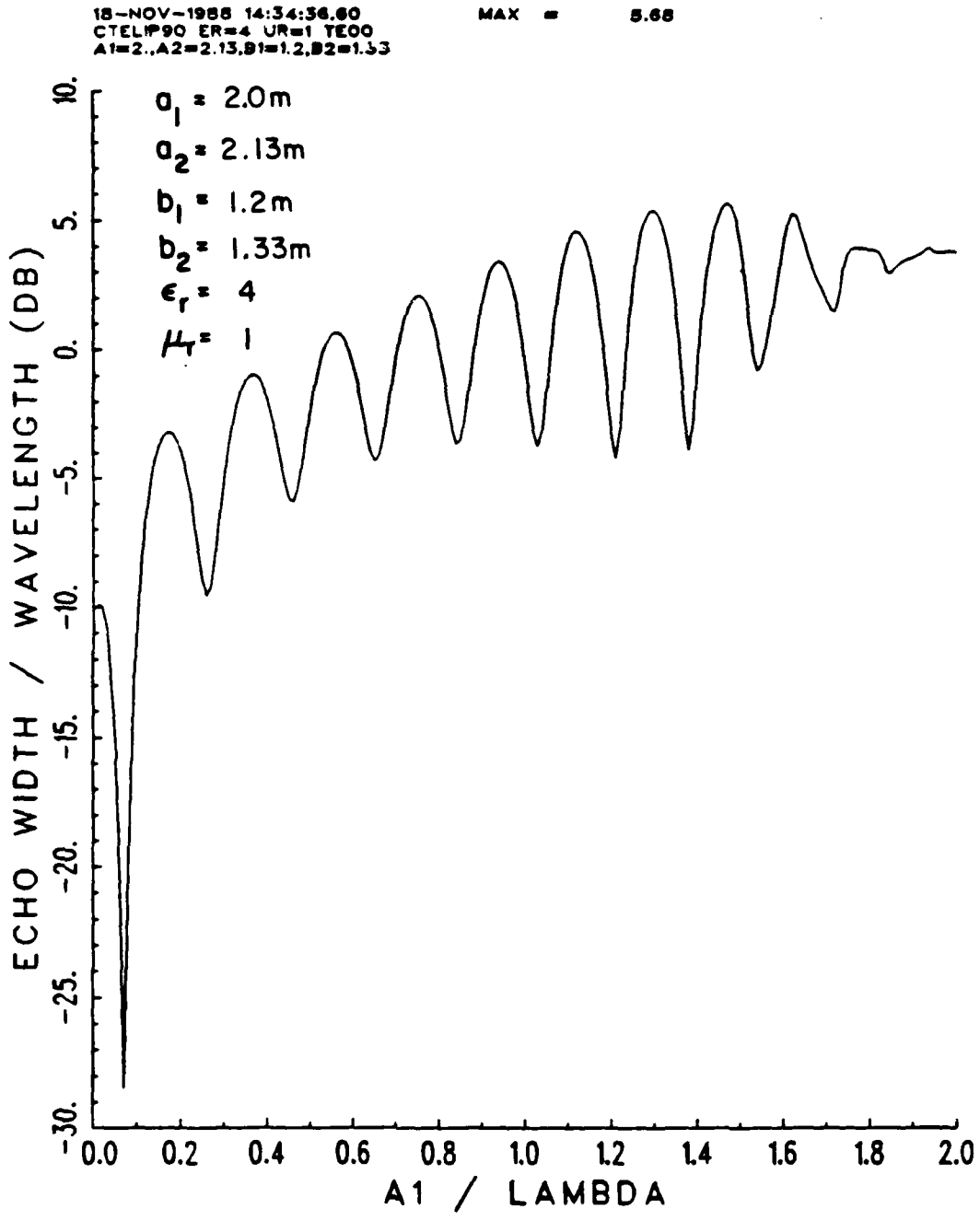

Figure 7: Backscatter for elliptic cylinder with uniform dielectric coating, TE polarization; $\phi_i = 0°$.

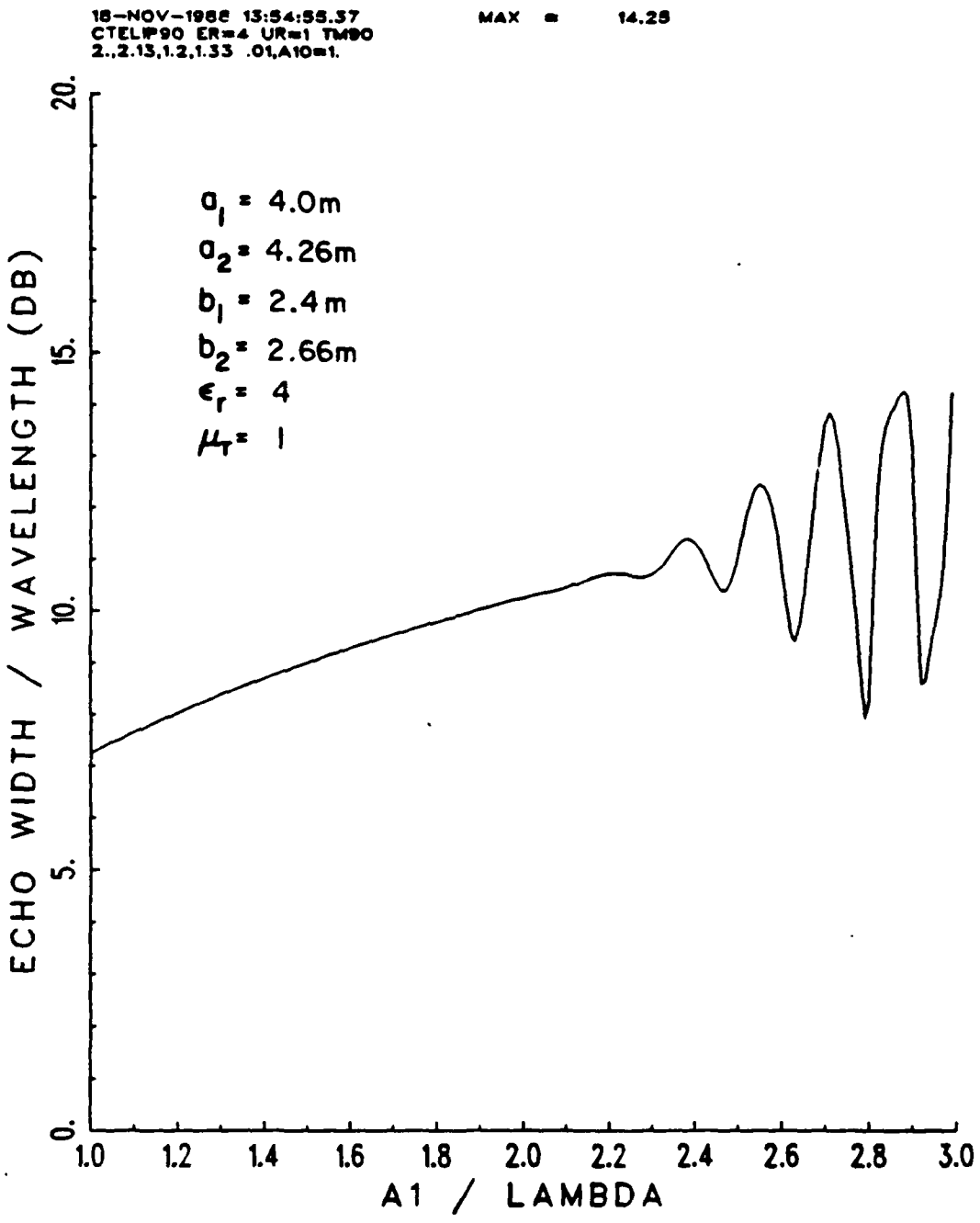

Figure 8: Backscatter for elliptic cylinder with uniform dielectric coating, TM polarization; $\phi_i = 90°$.

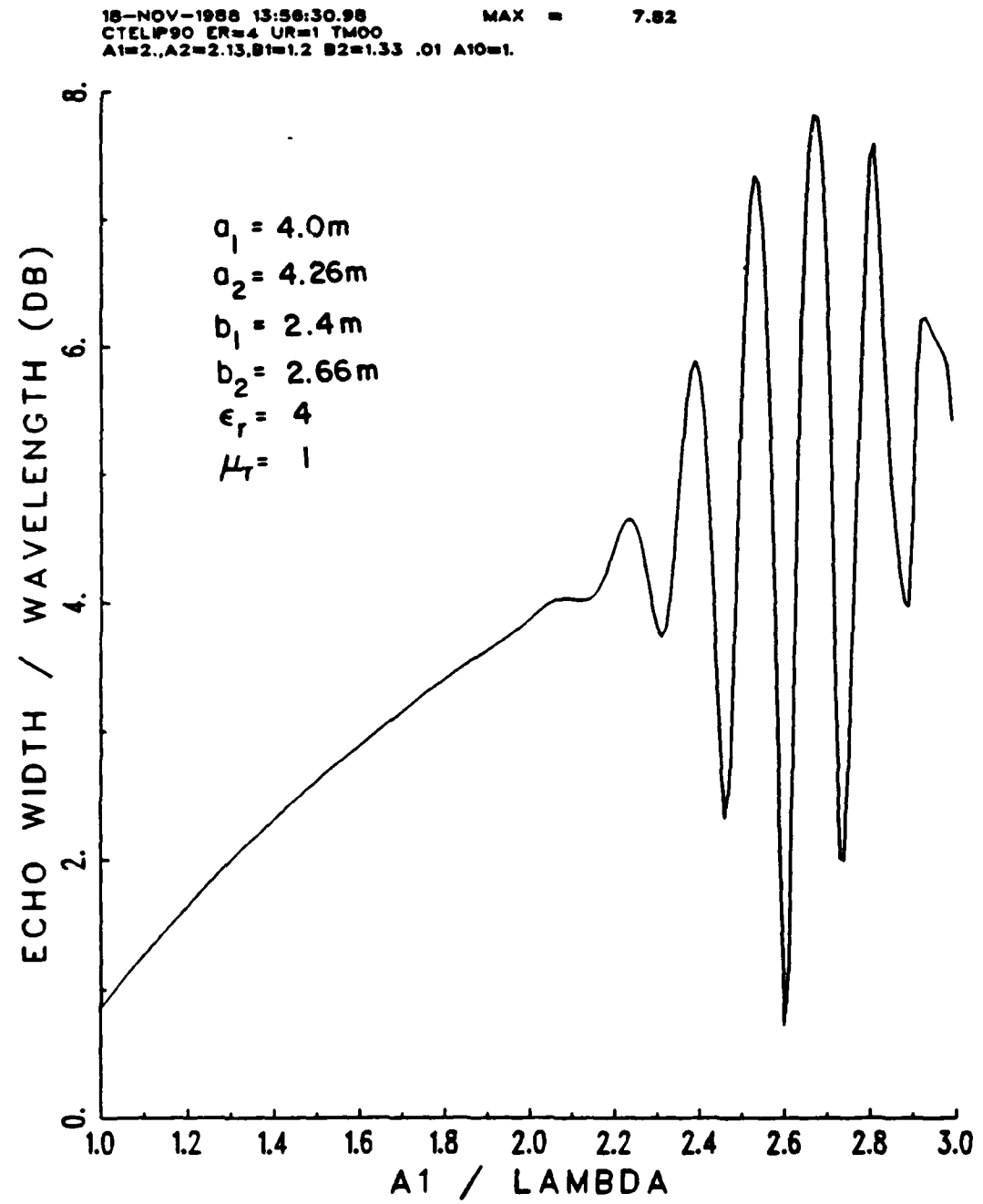

Figure 9: Backscatter for elliptic cylinder with uniform dielectric coating, TM polarization; $\phi_i = 0°$.

a single integral equation with only the external equivalent g_o as the independent unknown. Finally, the solution to the resulting integral equation has been obtained by the method of moment using a Pulse-Galerkin (delta-δelta) formulation. As a consequence, the elements of the matrix equation are simple to evaluate. Some preliminary results have been shown to be in agreement with those obtained by other approaches, e.g., the eigenfunction solution for the coated elliptic cylinder.

7. Reference

[1] J.H. Richmond "Scattering by a Conducting Elliptic Cylinder with Dielectric Coating," *Radio Science*, Vol. 23, No. 6, Nov.-Dec. 1988.

8. List of Papers - JSEP Diffraction Studies

Published:

1. R.G. Rojas, "Comparison Between Two Asymptotic Methods," *IEEE Transactions on Antennas and Propagation*, Vol. AP-35, No. 12, December 1987.

2. R. Paknys and N. Wang, "Excitation of Creeping Waves on a Circular Cylinder with a Thick Dielectric Coating," *IEEE Transactions on Antennas and Propagation*, Vol. AP-35, No. 12, pp. 1487-1489, December 1987.

3. R.G. Rojas, "Weiner-Hopf Analysis of the EM Diffraction by an Impedance Discontinuity in a Planar Surface and by an Impedance Half-Plane," *IEEE Transactions on Antennas and Propagation*, Vol. AP-36, No. 1, pp. 71-83, January 1988.

4. R.G. Rojas, "Scattering by an Inhomogeneous Dielectric/Ferrite Cylinder of Arbitrary Cross-Section Shape – Oblique Incidence Case," *IEEE Transactions on Antennas and Propagation*, Vol. AP-36, No. 2, pp. 238-245, February 1988.

5. R.G. Rojas, "Electromagnetic Diffraction of an Obliquely Incident Plane Wave Field by a Wedge with Impedance Faces," *IEEE Transactions on Antennas and Propagation*, Vol. AP-36, No. 7, pp. 956-970, July 1988.

6. R.G. Rojas, "Generalized Impedance Boundary Conditions for EM Scattering Problems," *Electronics Letters*, Vol. 24, No. 17, pp. 1093-1094, August 18, 1988.

7. P.H. Pathak, "Techniques for High-Frequency Problems," in Antenna Handbook (Theory, Applications and Design), ed. Y.T. Lo and S.W. Lee, (0-442-25843-7), Van Nostrand Reinhold Publishers, New York, 1988.

8. R.G. Kouyoumjian, section on RCS in Antenna Theory, J.D. Kraus, McGraw-Hill Publishers, New York, 1988.

Accepted for Publication:

1. L. Ersoy and P.H. Pathak, "An Asymptotic High Frequency Analysis of the Radiation by a Source on a Perfectly Conducting Convex Cylinder with an Impedance Surface Patch," *IEEE Transactions on Antennas and Propagation.*

2. R. Rojas and P.H. Pathak, "Diffraction of EM Waves Normally Incident on the Edge of a Thin Dielectric/Ferrite Half-Plane and Related Configurations," *IEEE Transactions on Antennas and Propagation.*

3. A.K. Dominek and L. Peters, Jr., "RCS Measurements of Small Circular Holes," *IEEE Transactions on Antennas and Propagation.*

4. O.M. Buyukdura, S.D. Goad and R.G. Kouyoumjian, "A Spherical Wave Representation of the Dyadic Green's Function for a Wedge," *IEEE Transactions on Antennas and Propagation.*

5. R. Tiberio, R. Manara, G. Pelosi and R.G. Kouyoumjian, "High Frequency EM Scattering of Plane Waves from Double Wedges," *IEEE Transactions on Antennas and Propagation.*

6. R. Tiberio, G. Pelosi, R. Manara and P.H. Pathak, "High Frequency Scattering from a Wedge with Impedance Faces Illuminated by a Line Source," *IEEE Transactions on Antennas and Propagation.*

7. P.H. Pathak and M.C. Liang, "On a Uniform Asymptotic Solution Valid Across Smooth Caustics of Rays Reflected by Smoothly Indented Boundaries," *IEEE Transactions on Antennas and Propagation.*

8. C.W. Chuang and M.C. Liang, "A Uniform High Frequency Asymptotic Analysis of the Diffraction by an Edge in a Curved Screen for Near Grazing Incidence," *J. Radio Science.*

9. R. Tiberio, G. Pelosi, G. Manara and P.H. Pathak, "A UTD Diffraction Coefficient for a Wedge with Impedance Faces Illuminated by a Line Source," *J. Radio Science.*

Submitted for Publication:

1. R. Rojas and Z. Al-Hekail, "Generalized Impedance/Resistive Boundary Conditions for EM Scattering Problems," *Radio Science*, August 1988.

2. H.T. Kim and N. Wang, "UTD Solution for the Electromagnetic Scattering by a Circular Cylinder with Thin Lossy Coatings," *IEEE Transactions on Antennas and Propagation.*

Papers in Preparation:

1. K.C. Hill and P.H. Pathak, "A UTD Analysis of the Diffraction of Surface Rays by an Edge in an Edge in an Otherwise Smooth Convex Surface for Non-Grazing Angles of Incidence," *J. Radio Science.*

2. H. Ly, H. Shamansky and R.G. Kouyoumjian, "Closed Form Solutions for the Elements of the Voltage Matrix in the Moment Method Solution of Linear Antennas," *IEEE Transactions on Antennas and Propagation.*

3. R.G. Rojas, Ling Miao Chou and P.H. Pathak, "Generalized Impedance Boundary Conditions for the Diffraction by a Dielectric Half Plane on a Conducting Ground Plane," *J. Radio Science.*

4. R.G. Rojas and P.H. Pathak, "Diffraction by the Edge of a Thin Dielectric/Ferrite Half Plane and Related Configurations for the Case of Skew Incidence at the Edge," *IEEE Transactions on Antennas and Propagation.*

Conferences/Oral presentations:

1. P.H. Pathak and M.C. Liang, "On a Uniform Asymptotic Solution Valid Across Smooth Caustics of Rays Reflected by Smoothly Indented Boundaries," 1988 IEEE AP-S International Symposium and URSI Symposium in Syracuse, New York during June 6-10, 1988.

2. M.C. Liang, P.H. Pathak and C.W. Chuang, "A Generalized UTD Analysis of the Diffraction by a Wedge with Convex Faces to Include Surface Ray Effects and Grazing Angles of Incidence/Diffraction," 1988 IEEE AP-S International Symposium and URSI Symposium in Syracuse, New York during June 6-10, 1988.

3. R.G. Rojas, L.M. Chou and P.H. Pathak, "Diffraction by a Magnetic Dielectric Half-Plane Using Generalized Impedance/Resistive Boundary Conditions," 1988 IEEE AP-S International Symposium and URSI Symposium in Syracuse, New York during June 6-10, 1988.

4. N. Wang, "A Simple Pulse-Galerkin Formulation for the Scattering by a Coated Cylinder," 1988 IEEE AP-S International Symposium and URSI Symposium in Syracuse, New York during June 6-10, 1988.

5. S. Kato and N. Wang, "Scattering of a Plane Wave from a Coated Circular Cylinder at Oblique Incidence - GTD Solution," 1988 IEEE AP-S International Symposium and URSI Symposium in Syracuse, New York during June 6-10, 1988.

IV. INTEGRAL EQUATION STUDIES

Researchers:
J.H. Richmond, Professor (Phone: 614/292-7601)

E.H. Newman, Research Scientist (Phone: 614/292-4999)
Adjunct Associate Professor
J. Blanchard, Grad. Research Assoc. (Phone: 614/294-9279)
M. Kluskens, Grad, Research Assoc. (Phone: 614/294-9286)

1. Introduction

This section will review the past year's work in integral equation studies. Our past work has concentrated on developing moment method (MM), and in some cases finite difference, solutions to important classes of electromagnetic (EM) radiation and scattering problems. These solutions provided basic information and a computational capability applicable to such areas as antenna analysis/design and the control of radar cross section.

The increased use of penetrable materials on aerospace vehicles leads to requirements for more efficient analytic treatment of such configurations. We may list the following examples of penetrable geometries: the dielectric radome, ablation coatings, composite media, and ferrite absorbers.

To promote the understanding of penetrable objects, we have analyzed the scattering properties of the thin dielectric strip (1983), the conducting circular cylinder partially coated with a thin ferrite layer (1984), a thin curved ferrite strip (1985) and a ferrite coated sphere (1986). These studies, accomplished during recent annual reporting periods, have demonstrated the dominant role played by surface waves in scattering by penetrable bodies of this type.

2. Review of Past Year's Research

Below we will review the past year's work in integral equation studies. Our research includes an eigenfunction solution for scattering from a material coated parabolic cylinder, a novel finite difference solution, scattering by an arbitrary cross section chiral cylinder, a technique for reducing computer CPU time when performing a MM computation over a wide frequency range, and a tutorial example of the method of moments.

The scattering properties of a dielectric coated elliptic cylinder and the radiation properties of an axial slot antenna on a dielectric coated elliptic cylinder were investigated. In addition, we made significant progress in our study of the variational properties of the moment method. These accomplishments are outlined in the following sections.

3. Material Coated Edges

Over the past few years we have had a significant effort devoted to material coated edges. This work included MM/Green's function solutions for an arbitrary cross section, lossy, inhomogeneous, dielectric/ferrite cylinder coating the edge of a perfectly conducting half-plane [10,20], and a tapered resistive strip extension of a perfectly conducting parabolic cylinder [3,4]. As described in a recent tutorial article [5], these MM/Green's function solutions are extremely efficient since they require unknowns only in the coating region, and not on the half-plane or parabolic cylinder. The problem of scattering by a arbitrarily shaped coated edge was the subject of a recent M.Sc. thesis [6]. Much of the above work will be summarized in a special issue of the Proceedings of the IEEE on radar cross section (RCS) [7].

Except for the circular cross section (and the work reported by Prof.

Richmond in the next section for the coated elliptic cylinder) there are no known eigenfunction solutions for material coated perfectly conducting cylinders. Eigenfunction solutions are important canonical problems and can be used as check cases for numerical or asymptotic techniques. In the past year we developed an eigenfunction solution to the problem of TM or TE scattering by a material coated parabolic cylinder. The inner and outer surfaces of the coating are parabolic cylinders with the same focal line, and thus a solution is possible using the parabolic cylinder eigenfunctions. However, unlike the coated circular cylinder, the parabolic cylinder eigenfunctions in the coating and free space regions are not orthogonal. As a result, no exact term by term solution for the coefficients in the eigenfunction solution is possible. Thus, we employ the method of moments to set up a matrix equation which is solved for the coefficients in the eigenfunction expansion. For thin coating, represented by a surface impedance, an exact term by term solution is possible. The coated parabolic cylinder work is the subject of a journal article in preparation [8].

4. Scattering by Elliptic Cylinder with Dielectric Coating

In some aspects an elliptic cylinder can simulate the fuselage or a wing of an aircraft, and the Green's function is known rigorously (in terms of Mathieu functions) for the elliptic cylinder. Therefore the exact eigenfunction solution for plane-wave scattering by a perfectly conducting elliptic cylinder with infinite length has been programmed.

Although we recently published some results for scattering by a conducting sphere with a thin ferrite coating, no data have appeared for a coated elliptic cylinder. Therefore we have investigated the scattering by a dielectric coated elliptic cylinder illuminated by a plane wave. To permit

an eigenfunction solution, we let the dielectric interface have an elliptic cross-section with the same interfocal distance as that of the conducting cylinder. As illustrated in Figure 1 the semimajor and semiminor axes are denoted by a_1 and b_1 for the conducting elliptic cylinder, and a_2 and b_2 for the dielectric interface. It may be noted that the dielectric coating has a nonuniform thickness, as shown.

In the dielectric layer we expand the field as an infinite series of Mathieu radial functions of the Bessel type with coefficients C_n, plus an infinite series of Mathieu radial functions of the Neumann type with coefficients D_n. Although the constants C_n and D_n are unknowns, it is easy to adust their ratio in such a way as to force the tangential electric field to vanish at the conducting surface. In the exterior free-space region the incident plane-wave field is expanded as an infinite series of Mathieu radial functions of the Bessel type with known coefficients A_n, and the scattered field is expanded in radial functions of the Hankel type with unknown coefficients B_n.

When we enforce the boundary conditions at the air-dielectric interface, we obtain an infinite system of simultaneous linear equations involving an infinite set of unknown coefficients B_n, C_n and D_n. To solve these equations, we employ the angular Mathieu functions as the basis and testing functions and apply Galerkin's method.

For the TM polarization, Figure 10 illustrates the backscatter versus the semimajor axis a_1/λ_o, where λ_o denotes the wavelength in free space. To generate these data, we varied the frequency from 150 MHz at the left edge to 450 MHz at the right edge of the graph. In the low-frequency region surface waves cannot propagate in the coating, so the backscatter is a smooth function. As the frequency is increased, the lowest order surface wave begins to propagate. Then the surface-wave contribution goes

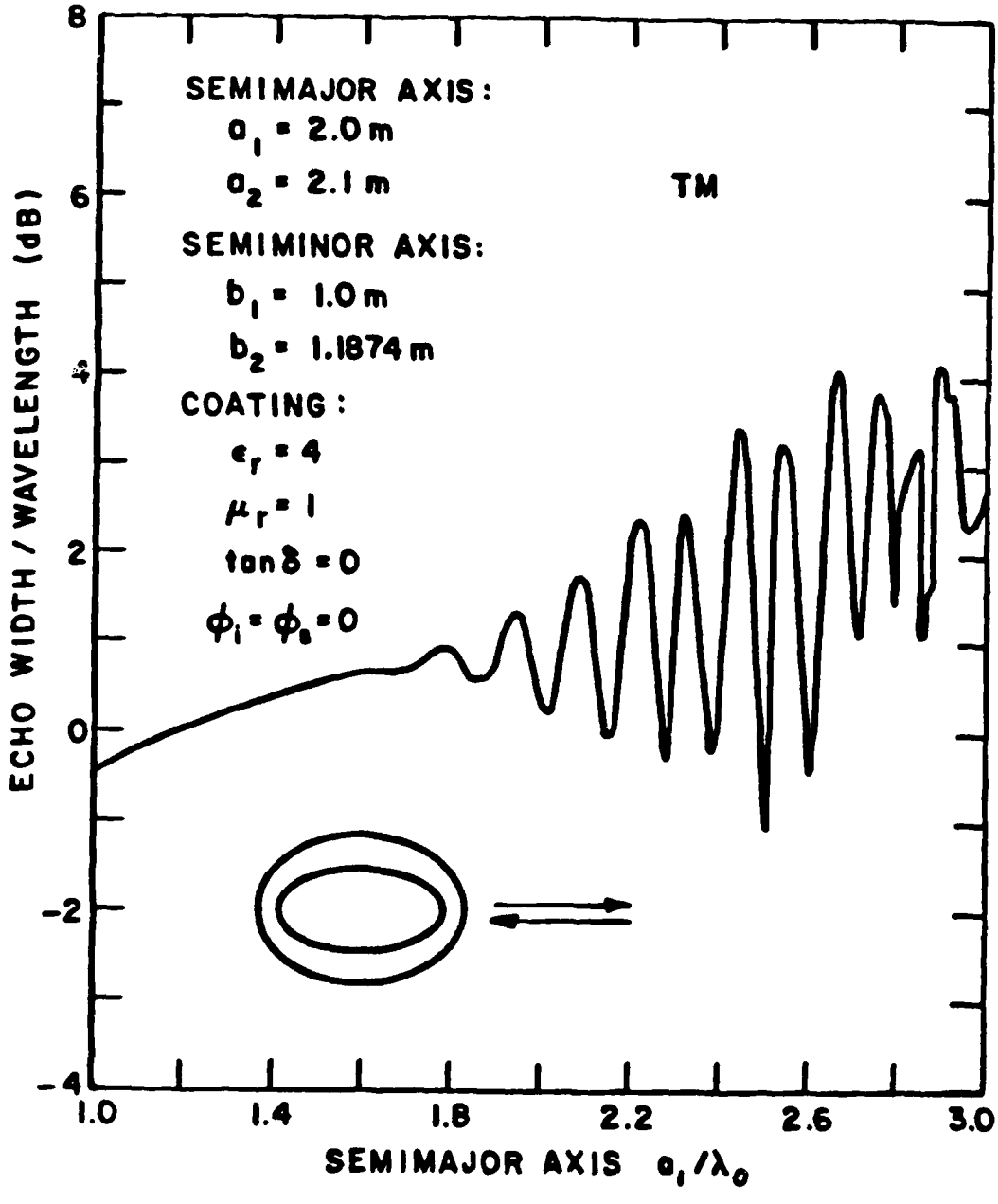

Figure 10: Backscatter versus semimajor axis for TM polarization.

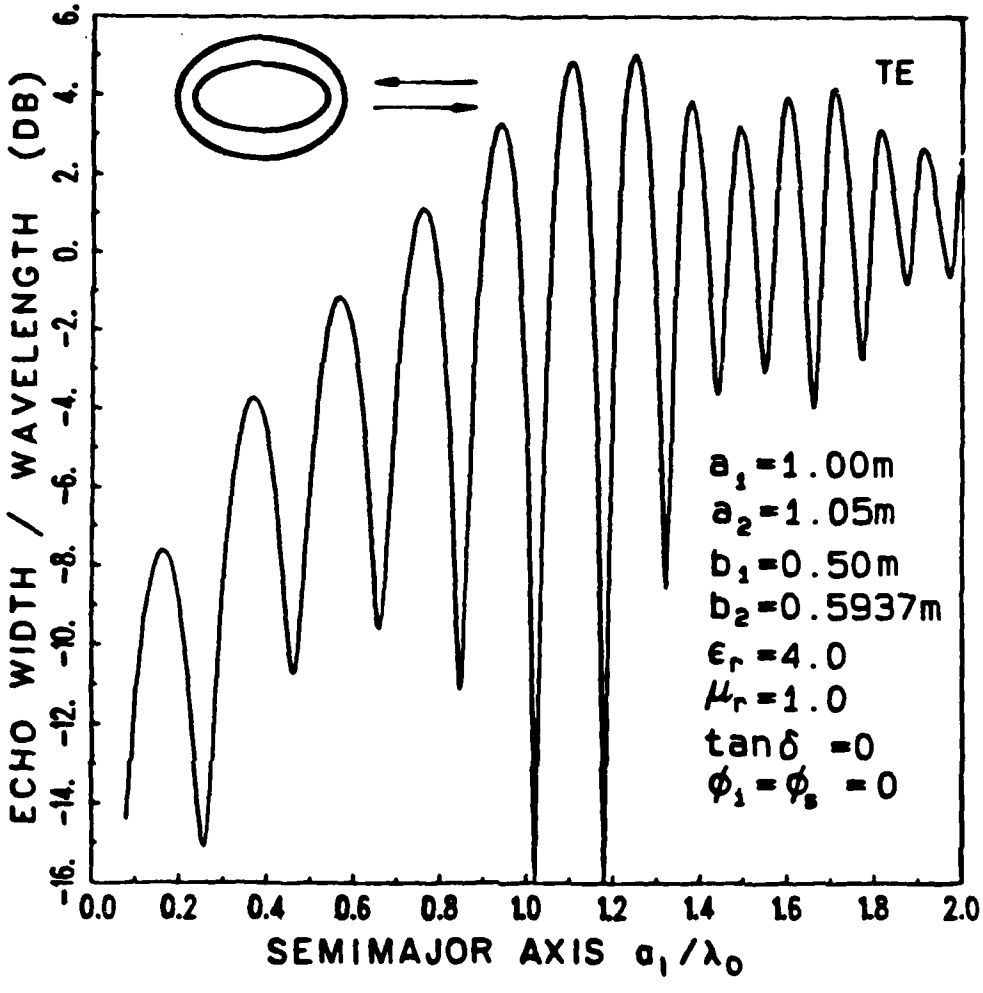

Figure 11: Backscatter versus semimajor axis for TE polarization.

alternately in phase and out of phase with the specular scattering term to produce the ripples shown in Figure 10. Figure 11 illustrates the analogous data for the TE polarization.

Our paper on this subject has been accepted for publication in *Radio Science*. The paper includes graphical data on bistatic scattering patterns, as well as backscatter versus angle of incidence. Many of our new results

have been verified by Dr. N. Wang with asymptotic techniques and by Dr. E.H. Newman with moment methods.

5. Axial Slot Antenna on Coated Elliptic Cylinder

With techniques similar to those in the preceding section, we investigated the radiation properties of an axial slot antenna on a dielectric-coated elliptic cylinder. The geometry is shown in Figure 1. The slot has infinite length in the axial direction, but the width can be small or large and the center of the slot can be located at any point around the perimeter of the cylinder. As is often done, the aperture field distribution is assumed uniform for the TE polarization and cosine for the TM polarization.

Figure 12 illustrates the radiation patterns for a narrow TM axial slot on an elliptic cylinder with $a_1 = \lambda_o$ and $b_1 = 0.5\lambda_o$. The center of the slot is located where the positive y axis intersects the conducting cylinder. The dielectric coating is lossless with $\mu_r = 1$ and $\epsilon_r = 4$. Let t denote the coating thickness at the center of the slot. Figure 12 illustrates the smooth radiation pattern with a thin coating ($t = 0.15\lambda_o$) such that the surface wave is highly attenuated as it propagates around the perimeter of the cylinder, and also the highly rippled pattern with a thicker coating ($t = 0.25\lambda_o$) such that the surface wave propagates with small attenuation. Figure 13 illustrates the corresponding results for the TE polarization.

We wrote a paper on this subject and submitted it for publication. In addition to the radiation patterns, this paper presents graphical results on the aperture conductance versus coating thickness, and the on-axis gain versus coating thickness.

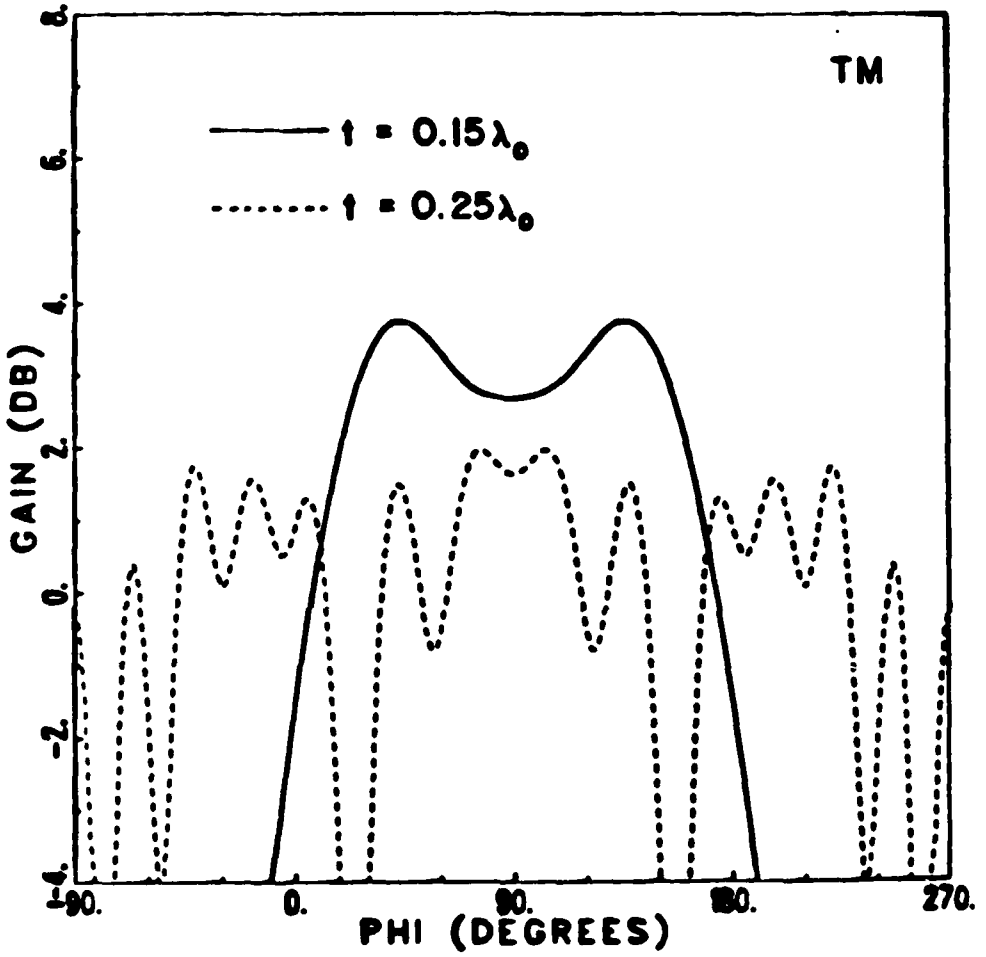

Figure 12: Radiation patterns for TM axial slot on coated elliptic cylinder.

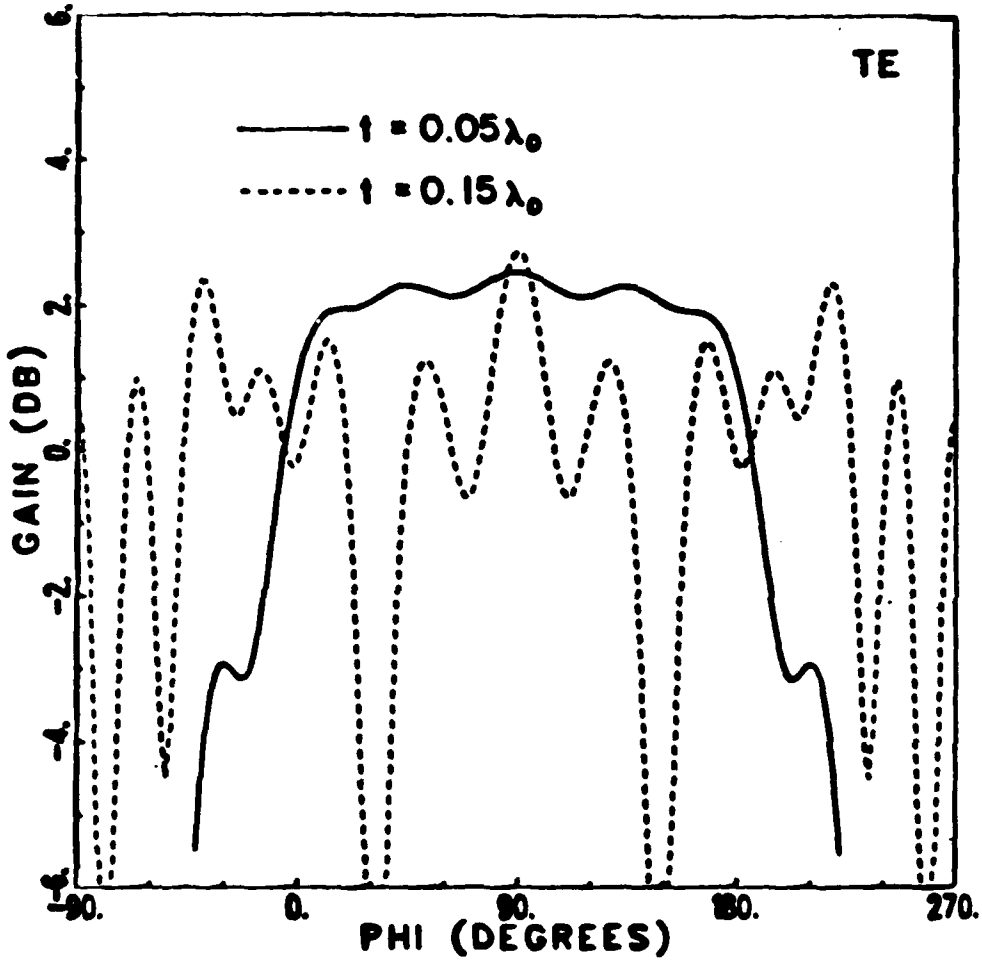

Figure 13: Radiation patterns for TE axial slot on coated elliptic cylinder.

6. On the Variational Properties of the Moment Method

Rather than devoting all our efforts to solving new geometries, we should occasionally consider improvements in our basic techniques for solving electromagnetic problems. In this contract period we made significant advances in our investigation of the variational properties of the moment method. This study will be completed early in the next period, and a paper will be submitted for publication. In antenna and scattering calculations, this research points toward improved accuracy with very little increase in computational costs.

7. Finite Difference Research

Most of our research has dealt with MM solutions of *integral equations* describing the radiation or scattering from a body. However, we are now beginning a study of a novel finite difference solution of the wave equation, i.e., a *differential equation* which describes the radiation or scattering from a body. Our solution will be limited to two dimensional bodies.

In a conventional finite difference solution for a cylinder of arbitrary cross section shape, one must determine a complicated grid of points surrounding the body at which the finite difference approximations to the derivatives will be computed. By contrast, in our method we begin by transforming the boundary of the arbitrary cylinder into a circular cylinder. Obtaining the finite difference grid for the circle in the transform space is much easier than for the general cross section cylinder in real space. The (transformed) differential equation will then be solved by the finite difference technique in the transform space. Once this solution in the transform space is obtained, the inverse transform must be applied to obtain the desired solution in real space.

8. Chiral Media

Regardless of the media, electromagnetics is governed by Maxwell's equations:

$$\begin{aligned} \nabla \times \mathbf{E} &= -\frac{\partial \mathbf{B}}{\partial t} \\ \nabla \times \mathbf{H} &= \mathbf{J} + \frac{\partial \mathbf{D}}{\partial t}. \end{aligned} \tag{1}$$

The properties of the media enter through the constitutive relations. For a regular medium,

$$\begin{aligned} \mathbf{D} &= \epsilon \mathbf{E} \\ \mathbf{H} &= \frac{\mathbf{B}}{\mu}. \end{aligned} \tag{2}$$

Here (μ, ϵ) are the permeability and permittivity of the media. If (μ, ϵ) are simple constants, then the media is linear, homogeneous, and isotropic. For a chiral media, the constitutive relations of Equations 2 are generalized to (time harmonic excitation assumed)

$$\begin{aligned} \mathbf{D} &= \epsilon \mathbf{E} + j\zeta \mathbf{B} \\ \mathbf{H} &= \frac{\mathbf{B}}{\mu} + j\zeta \mathbf{E}, \end{aligned} \tag{3}$$

where ζ is referred to as the chiral parameter.

We have begun research to analyze the scattering from a chiral cylinder of arbitrary cross section shape, using integral equation and method of moments (MM) techniques. The first step is to develop a volume equivalence theorem for chiral media. This theorem can then be used to obtain a set of coupled integral equations for the equivalent volume currents representing the chiral cylinder. These coupled integral equations will be solved for the equivalent currents using the MM. Once these currents are known, such quantities as the scattered fields or the fields in the chiral cylinder can be found in a fairly straight forward manner.

9. Nonlinear Media

We will consider a time-harmonic plane wave to have oblique incidence on a periodic planar array of parallel wire dipoles with nonlinear loads. The load may be series-opposing diodes to represent a nonlinear capacitor, or parallel-opposing diodes to represent a nonlinear resistor. In the steady state condition the scattered field will be periodic in space and time, and we have extended Floquet's theorem to cover this situation.

10. Other Miscellaneous Topics

In addition to the above described research, we have worked on the following problems:

1. We have developed a technique for interpolating the elements in the MM impedance matrix (as a function of frequency) which reduces the CPU time in performing a MM computation over a wide frequency bandwidth [9].

2. We have developed a simple MM solution for a short dipole which can be worked in about one hour using only a scientific calculator. Example problems based upon this solution should be useful in introducing a student to the MM [10].

11. References

[1] E.H. Newman, "TM Scattering by a Dielectric Cylinder in the Presence of a Half-Plane", IEEE Trans. on Antennas and Propagation, Vol. AP-33, pp. 773-782, July 1985.

[2] E.H. Newman, "TM and TE Scattering by a Dielectric/Ferrite Cylinder in the Presence of a Half-Plane", IEEE Trans. on Antennas and Propagation, Vol. AP-34, pp. 804-812, June 1986.

[3] E.H. Newman and J. Blanchard, "TM Scattering by an Impedance Sheet Extension of a Parabolic Cylinder", IEEE Trans. on Antennas and Propagation, Vol. AP-36, pp. 527-534, April 1988.

[4] E.H. Newman and J. Blanchard, "Numerical Generation of Parabolic Cylinder Functions", IEEE Trans. on Antennas and Propagation, scheduled for publication, April 1988.

[5] E.H. Newman, "An Overview of the Hybrid MM/Green's Function Method in Electromagnetics", Proc. of the IEEE, Vol. 76, March 1988, pp. 270-282.

[6] M. Kragalott, "Method of Moments Solution to Transverse Magnetic Scattering by a General Cylinder," M.Sc. thesis, Ohio State University, Dept. of Elec. Engr., August 1988.

[7] E.H. Newman and R.J. Marhefka, "Overview of MM and UTD Methods at the Ohio State University," Proc. of the IEEE, accepted for publication.

[8] E.H. Newman, "Plane Wave Scattering by a Material Coated Parabolic Cylinder," IEEE Trans. on Antennas and Prop., in preparation.

[9] E.H. Newman, "Generation of Wideband Data from the Method of Moments by Interpolating the Impedance Matrix", IEEE Trans. on Antennas and Propagation, scheduled for publication, December 1988.

[10] E.H. Newman, "Simple Examples of the Method of Moments in Electromagnetics", IEEE Trans. on Education, Vol. 31, pp. 193-200, August 1988.

12. List of Papers - JSEP Integral Equation Studies

Published:

1. E.H. Newman, "An Overview of the Hybrid MM/Green's Function Method in Electromagnetics," *Proceedings of the IEEE*, Vol. 76, No. 3, pp. 270-282, March 1988.

2. E.H. Newman, J.L. Blanchard, "TM Scattering by an Impedance Sheet Extension of a Parabolic Cylinder," *IEEE Transactions on Antennas and Propagation*, Vol. AP-36, No. 4, pp. 527-534, April 1988.

3. E.H. Newman, "Simple Examples of the Method of Moments in Electromagnetics," *IEEE Transactions on Antennas and Propagation*, Vol. AP-31, No. 3, pp. 193-200, August 1988.

4. E.H. Newman, section on Moment Methods in Antenna Theory by J.D. Kraus, McGraw Hill Publishers, New York, 1988.

Accepted for Publication:

1. J.H. Richmond, "Scattering by a Conducting Elliptic Cylinder with Dielectric Coating," *Radio Science.*

2. E.H. Newman, R.J. Marhefka, "Overview of Moment Method and Uniform Theory of Diffraction Method at the Ohio State University," *Proceedings of the IEEE.*

Submitted for Publication:

1. E.H. Newman and J. Blanchard, "Numerical Generation of Parabolic Cylinder Functions," *IEEE Transactions on Antennas and Propagation.*

2. E.H. Newman, "Generation of Wideband Data from the Method of Moments by Interpolating the Impedance Matrix," *IEEE Transactions on Antennas and Propagation.*

3. J.H. Richmond, "Axial Slot Antenna on Dielectric-Coated Elliptic Cylinder," *IEEE Transactions on Antennas and Propagation.*

Papers in Preparation:

1. E.H. Newman, "Plane Wave Scattering by a Material Coated Parabolic Cylinder."

2. E.H. Newman (edited by), *IEEE Press Collection of Reprints* "Application of the Moment of Methods in EM Radiation and Scattering."

3. J.H. Richmond, "On Variational Properties of the Moment Method."

Conferences/Oral Presentations:

1. E.H. Newman, "Generation of Wideband Data from the Method of Moments by Interpolating the Impedance Matrix," 1988 IEEE AP-S International Symposium and URSI Symposium in Syracuse, New York during June 6-10, 1988.

V. HYBRID TECHNIQUES

Researchers:
P.H. Pathak, Associate Professor (Phone: 614/292-6097)
R.C. Chou, Assistant Professor (Phone: 614/292-7298)
M. Marin, Fullbright Post-Doc. Fellow (Phone: 614/294-9286)
G. Zogbi, Grad. Research Assoc. (Phone: 614/294-9284)
M. Hsu, Grad. Research Assoc. (Phone: 614/294-9280)

1. Introduction

A goal of this research is to develop useful and efficient combinations of different hybrid techniques for analyzing a variety of electromagnetic (EM) radiation and scattering phenomena that would otherwise be either impossible or cumbersome to treat via any one technique.

During the past period, substantial progress has been made in the development of hybrid analysis for efficiently treating the EM phenomena associated with:

i. printed circuits/antennas, especially at high frequencies;

ii. scattering by shallow (antenna type) cavities; and

iii. scattering by deep (inlet type) cavities.

2. Development of Hybrid Techniques for Printed Circuits/Antennas

A uniformly asymptotic (high frequency) representation has been developed for the microstrip surface Green's function. This representation provides the fields in "closed form" near the surface of a single layer planar grounded substrate, and more recently also near a double layer planar grounded substrate-superstrate configuration, respectively, when they are excited by an electric point current source which is located on these planar

configurations. What is remarkable about this uniform asymptotic microstrip surface Green's function is that it remains accurate for distances from the source point which are as small as a few tenths of the free space wavelength. In contrast, a conventional exact integral representation of the microstrip surface Green's function becomes cumbersome and highly inefficient for source and field point separations near the surface which are more than a wavelength or so apart. A hybrid combination of the asymptotic microstrip Green's function with the MM integral equation technique which is developed here then allows one to very efficiently and accurately treat electrically large microstrip antenna phased arrays. Furthermore, the asymptotic microstrip Green's function provides a lot of physical insight as to the uniform behavior of the field within the transition region near the source, where the effects of proper and improper surface wave poles and leaky wave poles are explicitly shown to describe the near field effects. Specifically, the present analysis shows that while all proper and improper surface wave poles must be included at small distances from the source, the effects of other complex leaky wave poles are less significant and can be ignored in general. This explicit description of the effects of pole waves is not available in the exact integral representations for the microstrip Green's function. Such a physical insight provided by the explicit pole wave behavior in the asymptotic microstrip Green's function yields a simple means of studying the surface wave phenomenon with interesting applications to surface wave reduction or elimination (especially using the substrate-superstrate combination). Manuscripts describing these single and double layer asymptotic microstrip Green's functions have been submitted for publication. Also, a manuscript describing the evaluation of propagation constants of electrically narrow microstrip transmission lines

using the asymptotic microstrip Green's function has been accepted for publication. The above work now lays the foundation for the development of additional hybrid methods for predicting the effects of various types of stripline discontinuities (e.g., bends, couplers, etc.). In the latter hybrid approach, which will be developed in the next phase of this study, a set of traveling wave basis functions (with known propagation constants as indicated above) could be used to represent the unknown currents away from the stripline discontinuities, whereas, the usual subsectional basis functions could be employed at and near such discontinuities. The amplitudes of the current basis functions could then be found via the MM procedure which again employs the closed form asymptotic microstrip Green's function as described earlier. As a part of the future effort, it is also proposed to extend the above methods to anisotropic substrates (to model composite materials) and to cylindrically curved surfaces for conformal microstrip antennas.

3. Scattering by Shallow (Antenna type) Cavities

This topic has been and continues to be supported partially by JSEP. In the past, a novel hybrid approach for analyzing the scattering of an incident EM plane wave by dielectric loaded two-dimensional (2-D) cavities in a flat ground plane was developed. In that hybrid approach, the fields inside the dielectric filled cavity are represented by the set of parallel plate waveguide modes. The multiple scattering of waves between the open front end and the back end (short circuited termination) is taken into account via the self-consistent multiple scattering matrix method. The reflection and transmission scattering matrices for the open end are found via asymptotic high frequency methods; the reflection scattering matrix for the planar short circuit termination is well known. The use of asymptotic high frequency methods (such as the geometrical and physical theories of diffraction) lead

to relatively simple analytical expressions for the elements of the relevant scattering matrices; in contrast, a conventional mode matching technique leads to cumbersome and inefficient numerical solutions for these coefficients via matrix inversion. Thus, the present hybrid combination of modal and asymptotic high frequency method provides a useful and efficient analysis of the antenna cavity configuration. During the present period, that approach has been extended to include the effect of a simple waveguide fed slot in the back end of the cavity. The waveguide could be terminated in a load. A moment method (MM) based solution has been obtained for the slot aperture distribution to deduce the elements of the scattering matrices which characterize the reflection and transmission of waves at the slot aperture. These scattering matrices are independent of the incident angle. Presently, this result is being combined, again in a hybrid fashion with the analysis developed for the cavity without the slot to efficiently and accurately study the effect of the slot and the loading on the overall scattering by the cavity containing the waveguide fed slot. In the next phase of this study, an array of slots will be incorporated within the cavity; furthermore, the dielectric filling the cavity will be replaced by a thin dielectric radome or a frequency selective surface with known reflection characteristics in this generalization of the hybrid approach. Eventually, this hybrid approach will also be developed to treat 3-D situations involving rectangular and circular cavities in a planar surface, as well as by rectangular cavities in a cylindrical surface. In addition, it is proposed that these cavities will be allowed to contain more general antenna types than is presently possible.

4. Scattering by Deep (Inlet Type) Cavities

A hybrid modal approach was developed previously with partial support from JSEP to study the EM plane wave scattering by 2-D and 3-D inlet

type cavities which can be modeled (or built up) by joining together sections of piecewise separable waveguide geometries for which the interior modal fields are known or can be obtained. In the past, this approach has yielded interesting and useful results for 2-D S-shaped open-ended waveguide cavities formed by connecting straight and annular waveguide sections. The modal reflection and transmission coefficients associated with the junctions formed by the connections of different waveguide sections are found efficiently via asymptotic high frequency methods (such as the geometrical and physical theories of diffractions, and the equivalent current methods). This hybrid asymptotic modal approach provides physical insight into the process of EM penetration and scattering associated with such inlet cavity configurations because it isolates the effects of each of the junctions. This hybrid technique also provided an important connection between the modes most strongly excited in the waveguide cavity for a given direction of incidence/scattering; this type of information is useful for controlling the scattering by such cavities. More recently, this hybrid method was extended, under partial JSEP support, to develop an analysis for predicting the scattering by 3-D S-shaped open ended metallic cavities built up from straight and annular sections of waveguides with a rectangular cross-section. While the termination in all of the S-shaped cavities treated thus far is a simple planer short circuit, work is under progress to ascertain how one can deal with more complex terminations. The latter would involve the development of a more general hybrid procedure if one also includes a cavity of relatively arbitrary shape which cannot be built up by combining piecewise separable waveguide sections. At present, a generalized ray expansion technique is therefore being developed as a possible method to treat inlet cavities of fairly general shapes. It will be determined, under

partial JSEP support how this technique can also be combined via a special hybrid scheme to deal with complex terminations within such cavities of relatively arbitrary shape.

5. List of Papers - JSEP Hybrid Studies

Published:

1. A. Altintas, P.H. Pathak, M.C. Liang, "A Selective Modal Scheme for the Analysis of EM Coupling Into or Radiation from Large Open-Ended Waveguides," *IEEE Transactions on Antennas and Propagation*, Vol. AP-36, No. 1, pp. 84-96, January 1988.

Accepted for Publication:

1. C.W. Chuang and P.H. Pathak, "Ray Analysis of Modal Reflection for Three-Dimensional Open-Ended Waveguides," *IEEE Transactions on Antennas and Propagation.*

2. A. Nagamune and P.H. Pathak, "An Efficient Plane Wave Spectral Analysis to Predict the Focal Region Fields of Parabolic Reflector Antennas for Small and Wide Angle Scanning," *IEEE Transactions on Antennas and Propagation.*

3. S. Barkeshli, P.H. Pathak and M. Marin, "An Asymptotic Closed From Microstrip Surface Green's Function for the Efficient Moment Method Analysis of Mutual Coupling in Microstrip Antenna Arrays," *IEEE Transactions on Antennas and Propagation.*

4. C.W. Chuang, "Generalized Admittance for a slotted Parallel Plate Waveguide," *IEEE Transactions on Antennas and Propagation.*

5. C.W. Chuang, P.H. Pathak, "Efficient Hybrid Combination of Asymptotic High Frequency and Modal Techniques for Analyzing the EM Scattering by Open Ended Semi-Infinite Circular and Rectangular Waveguides with Simple Interior Terminations," *IEEE Transactions on Antennas and Propagation.*

6. S. Barkeshli and P.H. Pathak, "A Useful Uniform Asymptotic Approximation for for the Planar Microstrip Green's Function," *IEEE Transactions on Antennas and Propagation.*

7. M. Marin, S. Barkeshli and P.H. Pathak, "Efficient Analysis of Planar Microstrip Geometries Using a Closed Form Asymptotic Representation of the Grounded Dielectric Slab Green's Function," *IEEE Transactions of Microwave Theory and Techniques.*

8. P.H. Pathak and A. Altintas, "An Efficient High Frequency Analysis of Modal Reflection and Transmission Coefficients for a Class of Waveguide Discontinuities," *J. Radio Science.*

Submitted for Publication:

1. K.D. Trott, P.H. Pathak and F. Molinet, "A Uniform GTD Type Analysis of EM Plane Wave Scattering by a Fully Illuminated Perfectly Conducting Cone," *IEEE Transactions on Antennas and Propagation.*

2. S. Barkeshli and P.H. Pathak, "Radially Propagating and Steepest Descent Path Representation of the Planar Microstrip Dyadic Green's Function," *IEEE Transactions on Antennas and Propagation.*

3. M. Marin, S. Barkeshli and P.H. Pathak, "On the Location of Surface and Leaky Wave Poles for the Grounded Dielectric Slab," *IEEE Transactions on Antennas and Propagation.*

4. M. Marin, S. Barkeshli and P.H. Pathak, "Efficient Analysis of Planar Microstrip Geometries Using a Closed-Form Asymptotic Representation of the Green's Function," *IEEE Transactions on Antennas and Propagation.*

5. P.H. Pathak and R.J. Burkholder, "Modal, Ray and Beam Techniques for Analyzing the EM Scattering by Open-Ended Waveguide Cavities," *IEEE Transactions on Antennas and Propagation.*

6. S. Barkeshli and P.H. Pathak, "An Efficient Exact Integral Representation for the Planar Microstrip Green's Function," *J. Radio Science.*

Papers in Preparation:

1. M.C. Liang, P.H. Pathak and C.W. Chuang, "An Analysis of the Scattering by an Open-Ended Dielectric Filled Cavity in a Ground Plane," *IEEE Transactions on Antennas and Propagation.*

2. R.J. Burkholder, C.W. Chuang and P.H. Pathak, "An Analysis of the EM Scattering by an S-Shaped Open Ended Waveguide with an Interior Termination," *IEEE Transactions on Antennas and Propagation.*

Conferences/Oral Presentations:

1. S. Barkeshli and P.H. Pathak, "An Efficient Moment Method Analysis of Finite Phased Arrays of Microstrip Dipoles Using an Asymptotic Closed Form Approximation for the Planar Microstrip Green's Function," 1988 IEEE AP-S International Symposium and URSI Symposium in Syracuse, New York, during June 6-10, 1988.

VI. ADAPTIVE ARRAY STUDIES

Researchers:

R.T. Compton, Jr., Professor	(Phone: 614/292-5048)
Frederick Vook, Grad. Research Assoc.	(Phone: 614/292-7094)
Jim Ward, Graduate Research Associate	(Phone: 614/292-2902)
Mario Fulan, Graduate Research Associate	(Now at Bell Laboratories)

1. Introduction

Under the JSEP support, we have done research in three topics related to adaptive arrays:

1. Nulling bandwidth,

2. Adaptive array performance in digital communication systems, and

3. Adaptive arrays in packet radio communication systems.

We have also done a small amount of research on neural nets for pattern recognition. We discuss these areas separately below.

2. Studies on Adaptive Array Bandwidth

An important problem with adaptive arrays [1] is that their performance deteriorates with interference bandwidth. The wider the bandwidth of an interference signal, the more difficult it is for an adaptive array to null it [2] [3].

Figure 14 illustrates this problem. It shows the output signal-to-interference-plus-noise ratio (SINR) for a two element adaptive array when an interference signal arrives from angle θ_i from broadside. (In Figure 14 the elements are isotropic and a half wavelength apart.) The desired signal has 0 dB

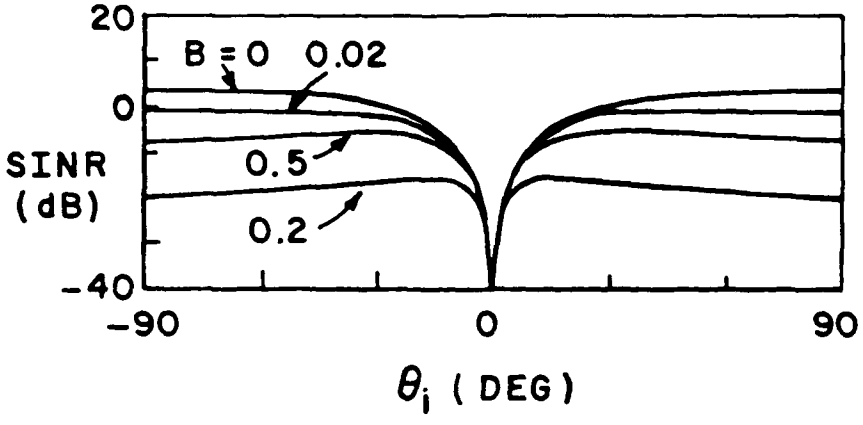

Figure 14: SINR versus θ_i: 2-element array, $\theta_d = 0°$, SNR=0 dB, INR=40 dB

signal-to-noise ratio (SNR) per element and arrives from broadside, and the interference has a 40 dB interference-to-noise ratio (INR) per element.) Figure 14 shows the SINR for several values of the relative bandwidth B, which is the ratio of the absolute bandwidth to the center frequency. As may be seen, for $B = 0.02$ the output SINR has dropped about 3 dB below its value for $B = 0$, and larger bandwidths cause increasingly more degradation. When the bandwidth performance of an adaptive array is inadequate, three methods exist for improving its performance:

1. Using more elements in the array,

2. Using tapped delay-lines behind the elements, and

3. Using fast Fourier transforms (FFT's) behind the elements.

Consider the typical performance obtained with each of these approaches.

If more elements are added to the array, the result is as shown in Figures 15(a)-15(d) for arrays with 3, 5, 10 and 20 elements. (Each array is a linear array with half wavelength spacing between elements; all parameters are the same as in Figure 14.) For each array the SINR is shown for $B = 0$ and $B = 0.2$. By comparing Figure 15 with Figure 14, it is seen that additional elements do improve the bandwidth performance. However, no matter how many elements are used, there is always a region for θ_i near θ_d where the SINR is poorer for $B = 0.2$ than for $B = 0$.

If tapped delay-lines are used behind the elements, the result is better. Figure 16 shows an adaptive array with a 2-tap delay-line behind each element. Figure 17 shows the SINR obtained with this array when the delay between taps is a quarter wavelength at the carrier frequency and when $B = 0.2$. Since the SINR in Figure 17 is essentially the same as that in Figure 14 for $B = 0$, adding the tapped delay-lines to the 2-element array has completely overcome the bandwidth degradation.

Now consider FFT processing. Figure 18 shows an adaptive array with FFT processing. An A/D converter takes samples of each element signal. When K samples have been taken from each element, they are transformed with an FFT. The FFT produces K frequency domain samples, which are multiplied by adaptive weights and then summed with corresponding samples from other elements. The array output signal is obtained from the inverse FFT of the weighted and summed frequency domain samples.

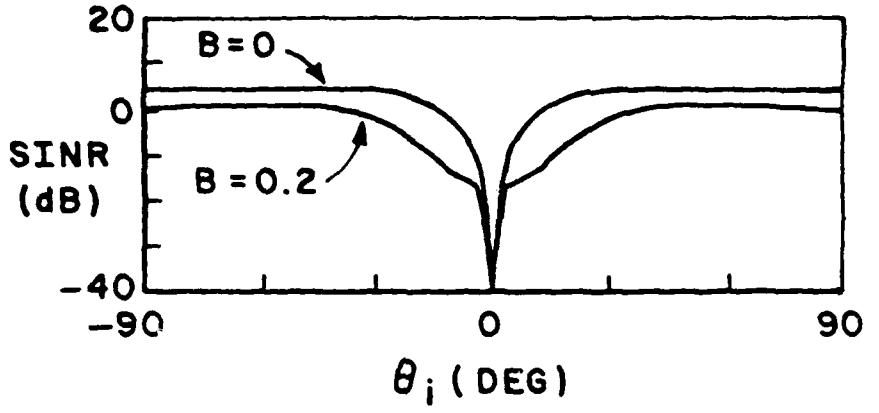

(a) 3 elements

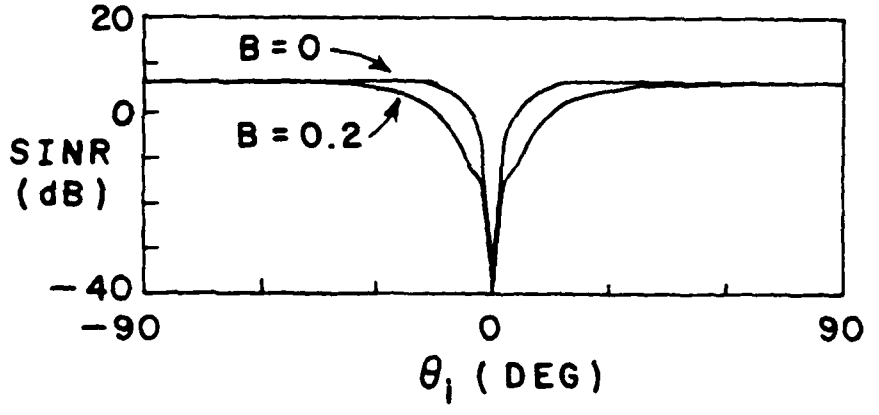

(b) 5 elements

Figure 15: SINR versus θ_i: $\theta_d = 0°$, SNR=0 dB, INR=40 dB

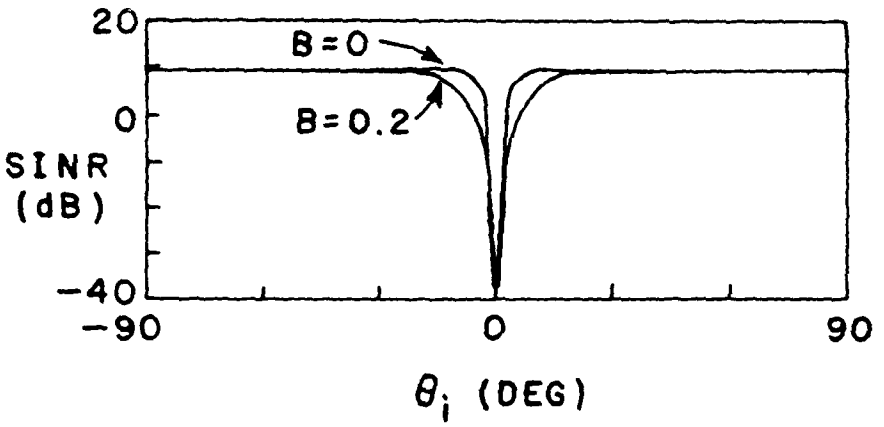

(c) 10 elements

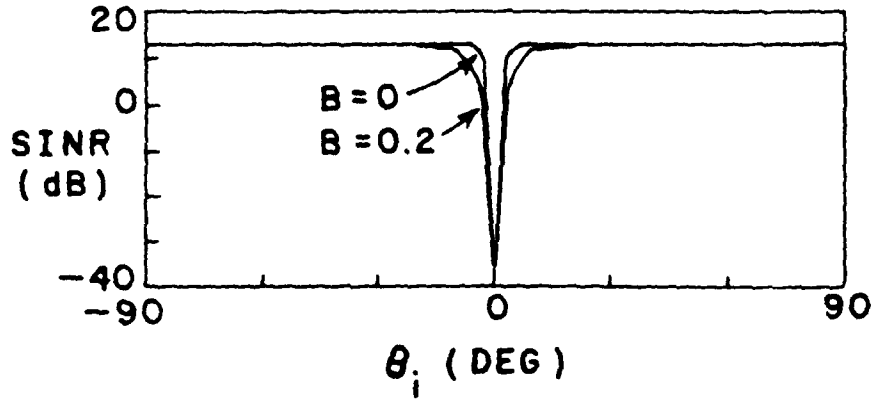

(d) 20 elements

Figure 15: Continued.

Figure 19 shows typical SINRs achieved with this arrangement. These curves are again computed for $B = 0.2$. The sampling rate for the A/D converters has been chosen to make one period of the FFT frequency response cover the signal bandwidth. Figure 19 shows the output SINR for $K = 2$, 4, 8 and 16 samples in the FFTs. As may be seen, the performance improves with K, the number of samples in the FFT, but it is never as good as the tapped delay-line performance shown in Figure 16.

Our purpose is studying the nulling bandwidth of adaptive arrays was twofold: (1) to understand how tapped delay-line and FFT parameters affect nulling bandwidth, and (2) to determine why FFT processing appears to give poorer results than tapped delay-line processing.

Our work in this area has resulted in two papers in the *IEEE Transactions on Antennas and Propagation* [4], [5], and we are currently preparing a third paper for publication [6]. The first paper [4] describes how the number of taps and the delay between taps affect the nulling bandwidth of a 2-element tapped delay-line array. The second paper [5] develops the basic relationship between tapped delay-line and FFT processing and shows that the two are actually equivalent. The performance differences seen in Figures 17 and 19 are entirely due to the fact that different sampling frequencies and different numbers of samples have been used in the two methods. The third paper [6], currently in preparation, describes the bandwidth performance of tapped delay-line arrays with more than 2 elements as a function of the delay-line parameters.

The work in references [4] and [5] was summarized in the JSEP Final Report of December 1986 [7]. In our summary here, we shall describe our work on nulling bandwidth subsequent to that report. Since December 1986, we have extended our results on the bandwidth performance of tapped

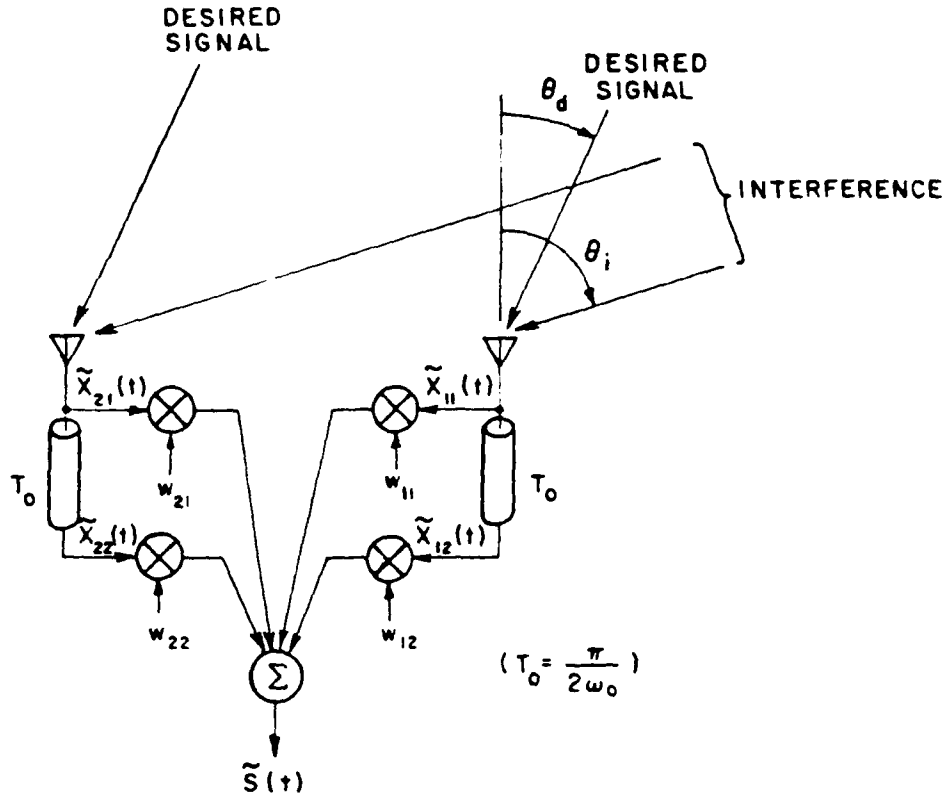

Figure 16: A 2-element array with 2-tap delay-lines

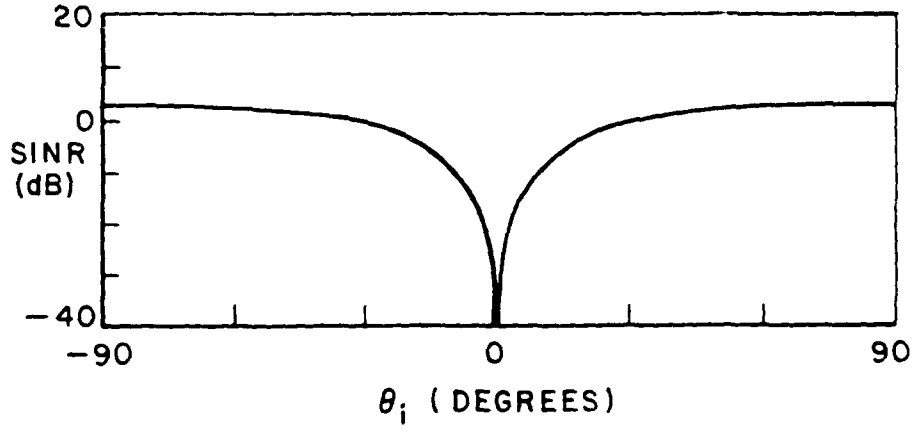

Figure 17: SINR versus θ_i: 2-taps per element, $\theta_d = 0°$, SNR=0 dB, INR=40 dB

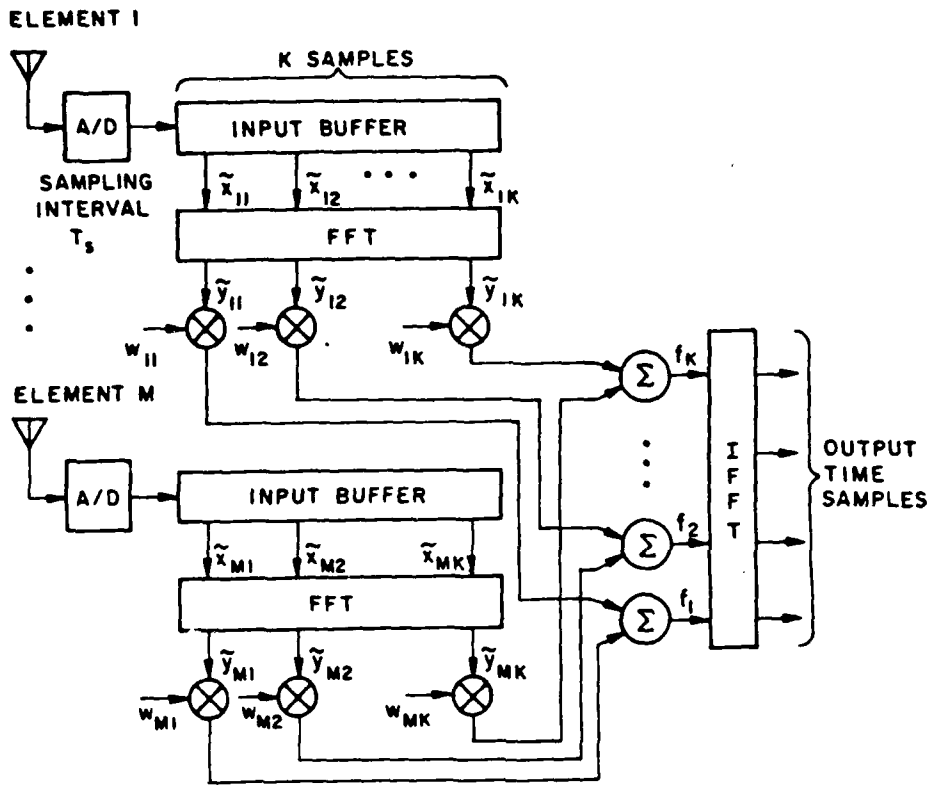

Figure 18: An Array with FFT Processing

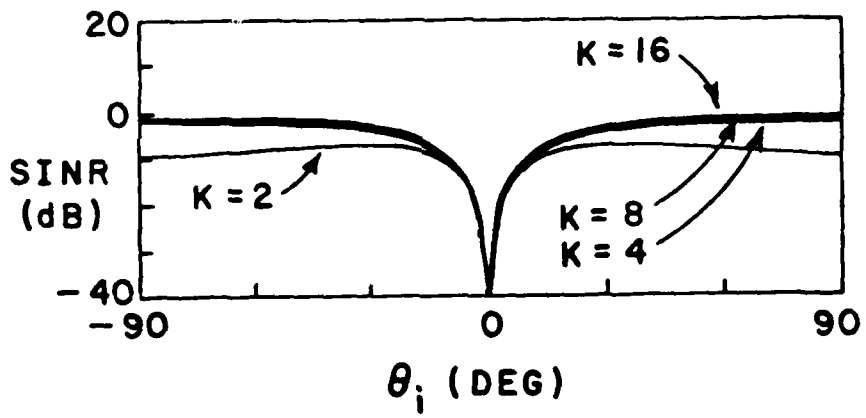

Figure 19: SINR versus θ_i: K-point FFT processing, B=0.2, $\theta_d = 0°$, SNR=0 dB, INR=40 dB

delay-line arrays by evaluating the bandwidth performance of linear arrays with up to 10 elements as a function of the number of taps and tap spacing behind each element. To evaluate an array with N elements, we assume that there are $N-1$ interfering signals incident on the array, all of the same bandwidth. From the SINR curves, for given bandwidths we have determined the delay-line configurations with the least number of taps that yield satisfactory performance for all interference arrival angles.

In this summary, we shall use a 3-element array to illustrate typical results. Figure 20 shows the performance of a 3-element array with a single complex weight behind each element as a function of the interference bandwidth. The SINR of the array is plotted as a function of the arrival angle of one interfering signal, θ_{i_1}. A second interference signal is also incident on the array from a fixed angle $\theta_{i_2} = 30°$. Each interfering signal has an INR of 40 dB per element. The SINR is shown for bandwidths of $B = 0$, 0.02, 0.05, and 0.2. Of course, the larger the bandwidth, the worse the SINR. For $B = 0.2$, the degradation is as large as 25 dB for some values of θ_{i_1}. (The sharp rise in SINR for $\theta_{i_1} \approx 30°$ occurs because only one degree of freedom is needed to null two interfering signals when they both arrive from the same angle.)

Figure 21 shows how the SINR changes if a single quarter wave delay and an extra weight is added behind each element (i.e., if there are two weights and one delay behind each element). The SINR is shown for $B = 0.01, 0.05$, 0.1, 0.15, and 0.2, with all other parameters the same as in Figure 207=. Note that the quarter wavelength delay and the extra weight behind each element has improved the performance dramatically. The performance is now equivalent to that obtained with CW signals for B up to 0.1.

If a second quarter wave delay and a third tap is added behind each

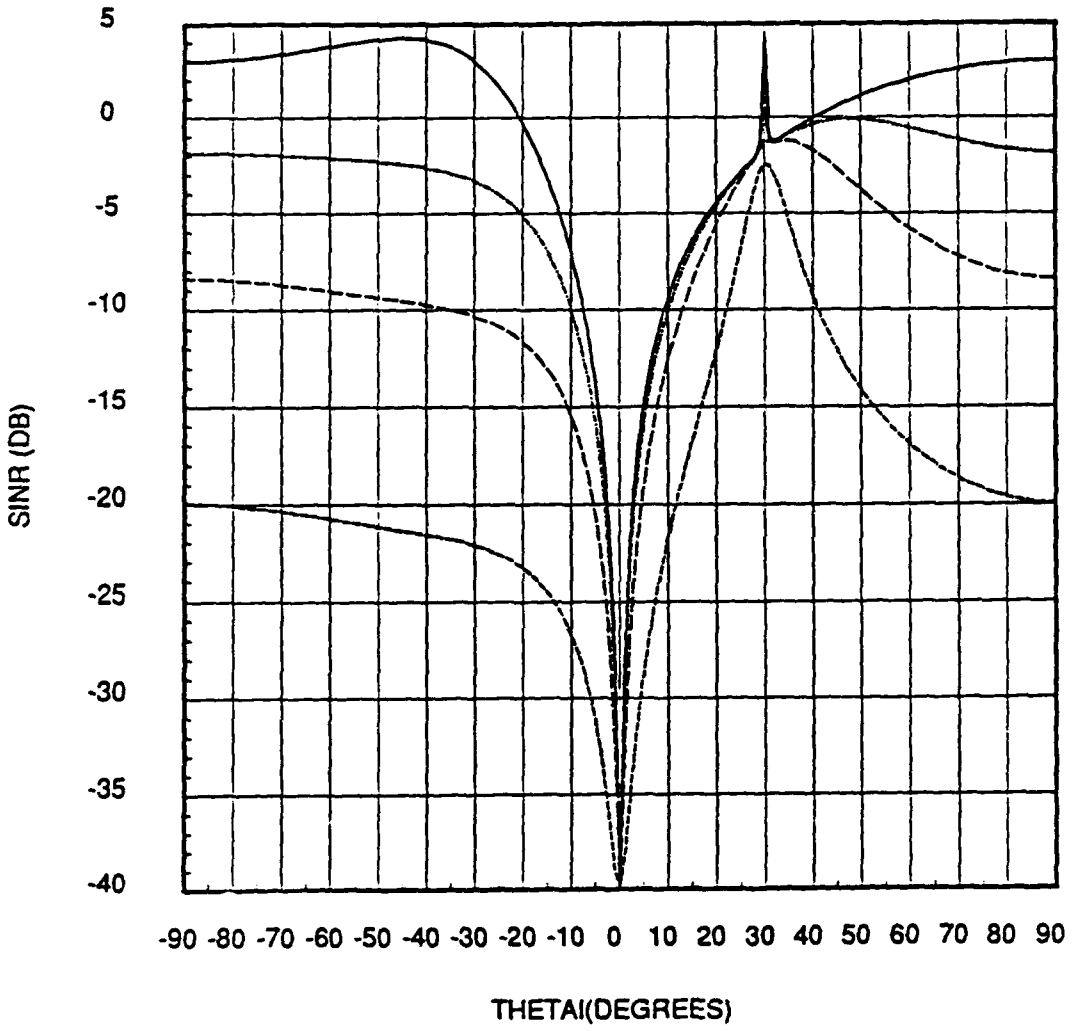

Figure 20: SINR versus θ_{i_1}: $\theta_d = 0°$, $\theta_{i_2} = 30°$, SNR=0 dB, INR1=INR2=40 dB

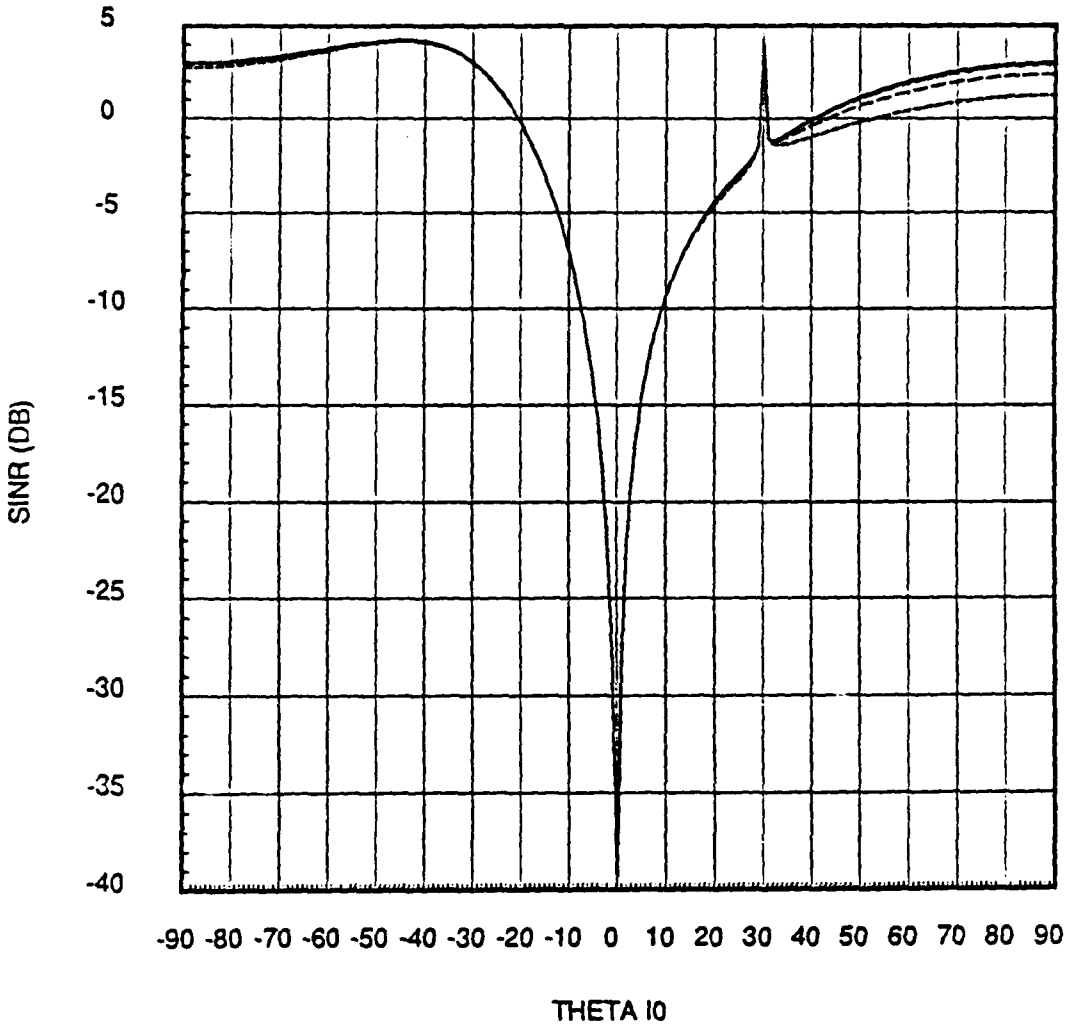

Figure 21: SINR versus θ_{i_1}: 2-tap delay-lines, $\theta_d = 0°$, $\theta_{i_2} + 30°$, SNR=0 dB, INR1=INR2=40 dB

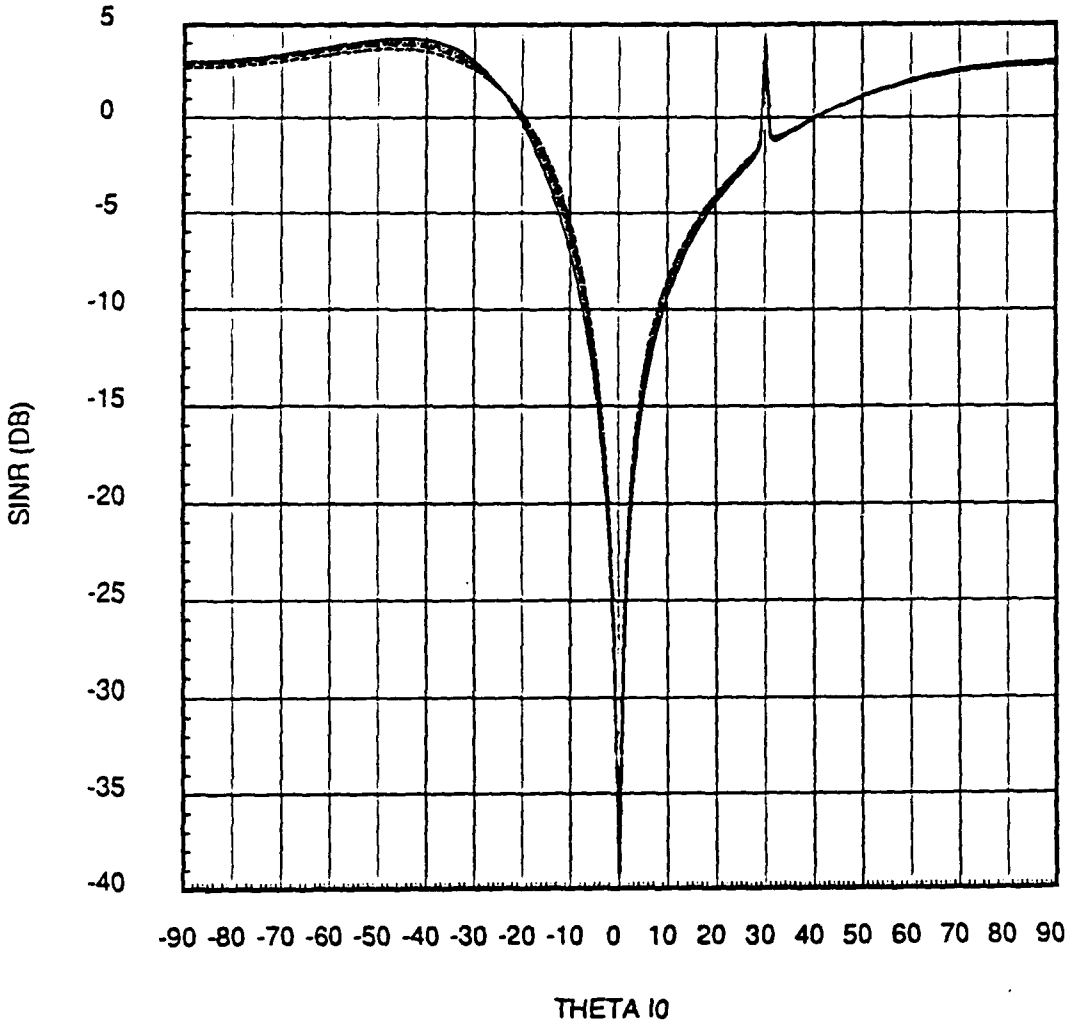

Figure 22: SINR versus θ_{i_1}: 3-tap delay-lines, $\theta_d = 0°$, $\theta_{i_2} + 30°$, SNR=0 dB, INR1=INR2=40 dB

element, the resulting SINR is shown in Figure 22. The SINR is now as good as that with CW signals for B up to 0.5. Thus, an additional delay and tap increases the useable bandwidth from 0.1 to 0.5.

The curves in Figures 21 and 22 are for the case where every element in the array has the same number of taps. However, it is also interesting to consider the case where different elements have different numbers of taps. To distinguish between different cases, we use the following notation. For an N-element array, we let K be a vector with N components, in which the i^{th} component is equal to the number of taps behind element i. For example, if $K = (2,1,1)$, we have an array with 3 elements, with 2 taps behind the left element and one tap each behind the middle and right elements. In addition, for a given set of taps, we define the *bandwidth cutoff* B_c to be the maximum bandwidth at which the array yields optimal performance for a particular arrangement of taps.

Table 2. shows the bandwidth cutoff B_c for various tap configurations for a 3-element array. These cutoff values were found by examining a large number of curves similar to Figures 21 and 22.

The data above were calculated for the case where the delay between delay-line taps is a quarter wavelength, an arbitrary choice. If one examines the performance of an array with a given number of taps as a function of the delay between taps, one finds that there is an optimal *range* of values for the intertap delay. Within this range, the performance is essentially constant. If the intertap delay is below the optimal range, the SINR does not drop but the array weights become very large. If the intertap delay is above the optimal range, the SINR drops. We refer to the maximum intertap delay that yields optimal performance as the *intertap delay cutoff*. Table 2 shows the intertap delay cutoff (in quarter wavelengths) for a 3-element adaptive

Bandwidth cutoff	K	B_c	K	B_c
3 element array	(1,2,1)	0.005	(3,2,1)	0.07
2 interfering signals	(2,1,1)	0.005	(2,3,1)	0.07
$\xi_{i_1} = \xi_{i_2} = 40$dB	(1,1,2)	0.005	(3,1,2)	0.005
$\xi_d = 0$dB	(2,1,2)	0.005	(3,2,2)	0.2
$r = 1$	(2,2,1)	0.05	(2,2,3)	0.2
	(1,2,2)	0.05	(2,3,2)	0.35
	(2,2,2)	0.1	(3,3,3)	0.5

Table 1: Bandwidth cutoffs for the 3-element array

Intertap Delay Cutoff	B	τ_c
3 element array	0.01	$200 = 2.0/B$
2 interfering signals	0.05	$30 = 1.5/B$
$\xi_{i_1} = \xi_{i_2} = 40$dB	0.10	$10 = 1.0/B$
$\xi_d = 0$dB	0.20	$5 = 1.0/B$
	0.3	$3 = 0.9/B$

Table 2: Intertap delay cutoffs for the 3-element array

array at different bandwidths.

In a similar way, we have examined the bandwidth performance of arrays with up to 10 elements. For arrays with more than 3 elements, we have found that for some combinations of interference angles, the bandwidth degradation of the array with large bandwidth signals cannot always be

fully overcome by adding more taps to the array. In these cases, as more taps are added, the SINR reaches a plateau that can be as much as 5 dB below the SINR obtained with CW signals. Adding more taps does not result in any significant improvement in the SINR, regardless of the delay between taps. This situation occurs only for certain combinations of interference angles, usually when one or two interfering signals arrive from endfire. Figure 23 shows an example of such a case, for a 5-element array with 4 interfering signals. The fixed interfering signals arrive from $-90°$, $10°$, and $+90°$, and all bandwidths are 0.2. Note that, for θ_{i_1} between $10°$ and $80°$, the SINR with three taps per element is 2 to 4 dB below the CW curve. Adding more than 3 taps per element does not significantly improve the SINR performance in this case.

Table 3 shows the bandwidth cutoff B_c for larger arrays as a function of the number of elements in the array and the number of taps behind each element. This table is for the case where every element in the array has the same number of taps. Table 4 shows the intertap delay cutoff (in quarter wavelengths) as a function of the number of elements and the bandwidth.

As mentioned above, we are currently preparing a paper for publication on the above results. (This work will also serve as a M.Sc. Thesis [8].)

3. Adaptive Array Performance in Digital Communication Systems

Our second area of work under JSEP was a study of the performance of adaptive arrays in digital communication systems. The purpose of this study was to determine the bit error performance of digital communication systems as a function of the adaptive array and jamming signal characteristics. Unlike earlier work on the performance of adaptive arrays against

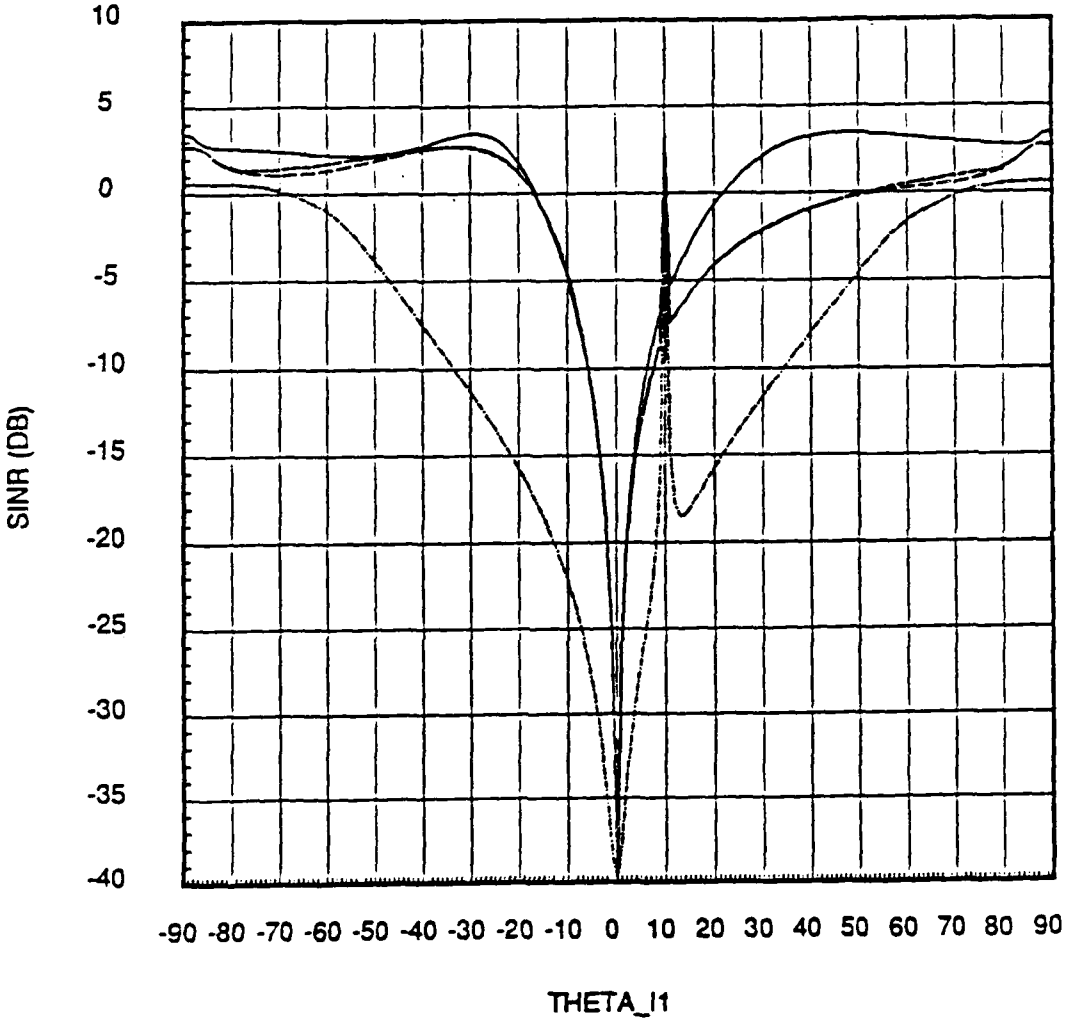

Figure 23: SINR versus θ_{i_1}: 5-elements, $\theta_{i_2} = 90°$, $\theta_{i_3} = -90°$, $\theta_{i_4} = 10°$, $\theta_d = 0°$, SNR=0 dB, All INR=40 dB, $B = 0.2$

Bandwidth cutoff M elements $M-1$ interfering signals, $\xi_i = 40$dB $\xi_d = 0$dB, r=1							
Taps	Number of Elements M						
Per Element	4	5	6	7	8	9	10
2	0.05	0.05	0.05	0.01	0.01	0.01	0.01
3	0.30	0.20	0.20	0.10	0.10	0.10	0.10
4	-	-	-	0.15	0.15	0.15	0.15

Table 3: Bandwidth cutoffs for M element arrays

Intertap Delay Cutoff r_c M elements $M-1$ interfering signals $\xi_d = 0$dB, $\xi_i = 40$dB				
Frac. BW	Number of Elements M			
B	$3 \leq M \leq 5$	$M = 6$	$M = 7, 8$	$M = 9, 10$
0.01	$200 = 2.0/B$	$150 = 1.5/B$	$150 = 1.5/B$	$150 = 1.5/B$
0.05	$30 = 1.5/B$	$20 = 1.0/B$	$20 = 1.0/B$	$20 = 1.0/B$
0.10	$10 = 1.0/B$	$10 = 1.0/B$	$10 = 1.0/B$	$9 = 0.9/B$
0.15	-	-	$6.5 \approx 1.0/B$	$6 = 0.9/B$
0.20	$5 = 1.0/B$	$5 = 1.0/B$	-	-

Table 4: Intertap delay cutoffs for M element arrays

jamming, these studies took signal and jammer waveforms into account as well as their powers.

Our studies in this area resulted in one Ph.D. dissertation [9], three papers in IEEE Transactions [10]-[12], a fourth paper accepted in the IEEE Transactions on Communications [13], and 2 conference papers [14],[15]. These papers describe the bit error probability of BPSK (binary phase shift keying), QPSK (quadriphase shift keying), binary DPSK (differential phase shift keying), and binary FSK (frequency shift keying) signals when received by adaptive arrays and subjected to CW and bandlimited gaussian noise jamming. Bit error probabilities are related to the desired signal and jammer spectral densities, powers, arrival angles, bandwidths, and also to the array bandwidth.

Since the results for this work were summarized in the JSEP final report of December 1986 [7], we shall not go into details here. The reader is referred to that report for further information.

4. Adaptive Arrays in Packet Radio

Under JSEP we have also studied the use of adaptive arrays in packet radio communication systems. We believe that the use of adaptive arrays can make a dramatic improvement in the operating characteristics of packet radio networks. In our studies, we have considered a simple packet radio system using an ALOHA protocol operating through a store-and-forward repeater. The adaptive array replaces the omnidirectional antenna usually assumed for the repeater. The benefit of the adaptive array is that it eliminates most packet collisions and thereby results in a great increase in throughput and a corresponding reduction in delay.

In an ALOHA packet radio system, stations transmit information to each other in the form of fixed length packets. Packets are sent from each

station to a central repeater, which then echos them back to the other stations in the net. Each station transmits a packet to the repeater whenever it has one to send, regardless of whether another station may be transmitting at the same time. Because individual users do not coordinate their transmissions, packets from different users frequently collide at the repeater. Packets are demodulated at the repeater and checked for errors, using an error detection code. If a packet is found to be error free, it is retransmitted back to the users in the net. If the packet suffered a collision, it will contain errors, which are detected at the repeater. In this case the repeater simply discards the corrupted packet. When an originating station does not hear its packet being repeated, it retransmits it after a random delay. Collisions limit the maximum throughput of a pure ALOHA system to 18% and a slotted ALOHA system to 36%.

In this work, we have studied the use of adaptive arrays as a way of improving this low throughput. The adaptive array is used as the receiving antenna at the repeater. The array improves the throughput and reduces delay in the packet system by acquiring a packet arriving from one angle and then nulling subsequent packets that arrive from other angles. In this way the array prevents interfering packets from destroying the acquired packet. The adaptive array allows one packet to get through, even when several packets are incident. As a result, the average throughput is higher than in a conventional packet system, for which there is no throughput when two packets collide. An adaptive array takes advantage of a previously unused parameter in a packet radio system: packet arrival angle.

This technique is an alternative to the approach known as Carrier Sense Multiple Access, or CSMA [16]. In CSMA, each station listens to the channel before transmitting, to determine if it is in use. If the channel

is busy, transmission is delayed until the channel becomes idle. Once the channel is idle, several strategies are possible for deciding when to transmit. The particular stategy used strongly affects the throughput of the packet system. By choosing the retransmission probability properly, very large throughputs are possible [16].

However, CSMA is applicable only to packet radio networks in which all stations can hear each other. If the stations cannot hear one another, CSMA does not work as well. The advantage of our adaptive array technique is that it does not require the stations in the net to be able to hear each other. Whether stations are within range of one another or not makes no difference with this technique.

In our studies, we have considered both slotted and unslotted ALOHA protocols. In a *slotted* system, a common time reference is maintained throughout the network. Time is segmented into well-defined intervals, or *slots*. Stations time their transmissions so every packet falls entirely within one slot. In an *unslotted* system, no system time is maintained. Stations simply transmit packets in a completely uncoordinated way.

The main difficulty in using an adaptive array in a packet radio system is the acquisition problem. Each packet to be received by the array arrives at an unknown time and from an unknown direction. It is necessary to focus the array pattern on a packet very quickly, in time to receive the message part of the packet. Our technique for doing this is as follows. We add a special two-part preamble to the beginning of every packet. The array pattern is locked onto the packet during this preamble. The first part of the preamble triggers the acquisition process, and the second part is used to form the beam on the packet.

Figure 24 shows how a packet is organized. A packet is formed by first

collecting a fixed number of message bits in a buffer. Then an address segment is added to the front of the packet, as shown in the top part of Figure 24. The address segment identifies the destination station and the originating station and may also contain other information needed to interpret the packet, such as a packet number. Next, the combined address and message segments are encoded with an (n, k) linear block code [17]. The k bits of the address and message segments are encoded into n bits in the final packet. This code is used for error detection or correction at the repeater. Finally, after encoding, an additional two-part preamble is added to the front of the packet. This two-part *acquisition preamble* is used to lock the array pattern onto the packet, as mentioned above. The packet bit stream is modulated on a carrier using a digital modulation such as BPSK (biphase shift keying) or binary FSK (frequency shift keying).

Packet acquisition by the array is done as follows. Whenever the repeater is ready to acquire a new packet, the array weights are set to give the array a pattern that covers all users in the net. (We call this the *uniform coverage* pattern.) Such a pattern is easily obtained by turning one array element on and the rest off. With one element on, the array pattern is just the pattern of that element. The element pattern for that element is chosen so it covers the entire net. With the uniform coverage pattern, any user can access the array.

The acquisition preamble contains two code sequences, called Codes 1 and 2, as shown in Figure 24. Code 1 is a short code with a highly peaked aperiodic autocorrelation function, such as a Barker code [18]. Figure 25 shows the aperiodic autocorrelation function of a 13-bit Barker code, for example. Code 2 consists of an integral number of periods of a pseudonoise (PN) code [19]. The (periodic) autocorrelation function of such a code has

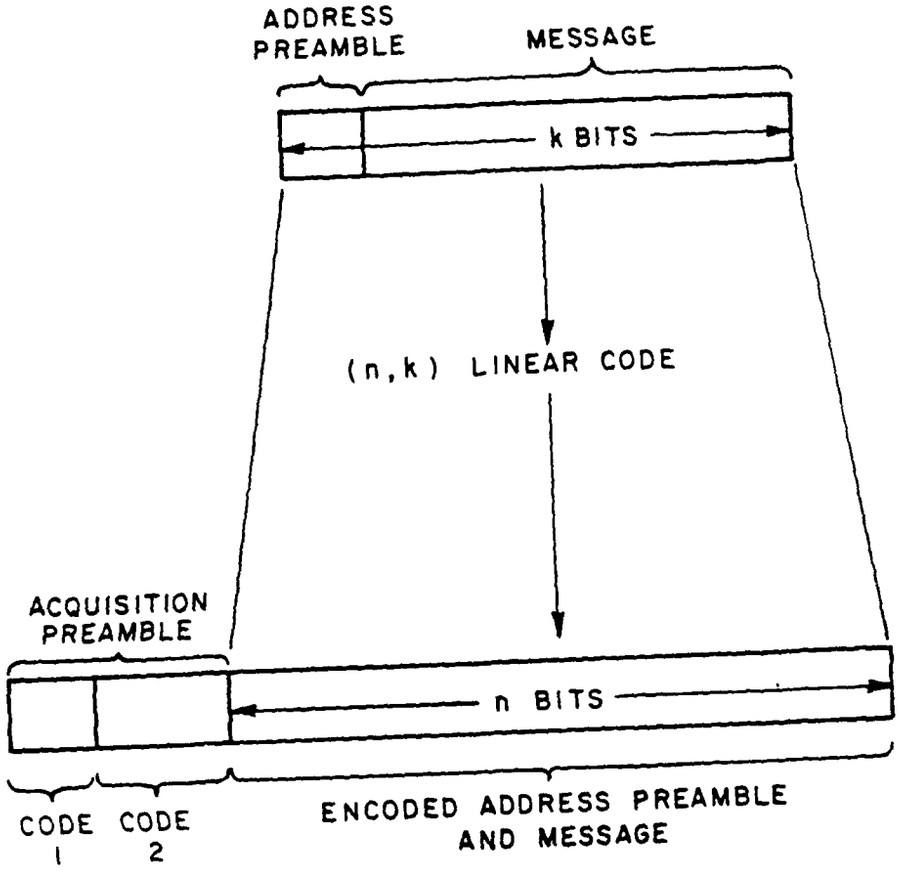

Figure 24: Packet Organization

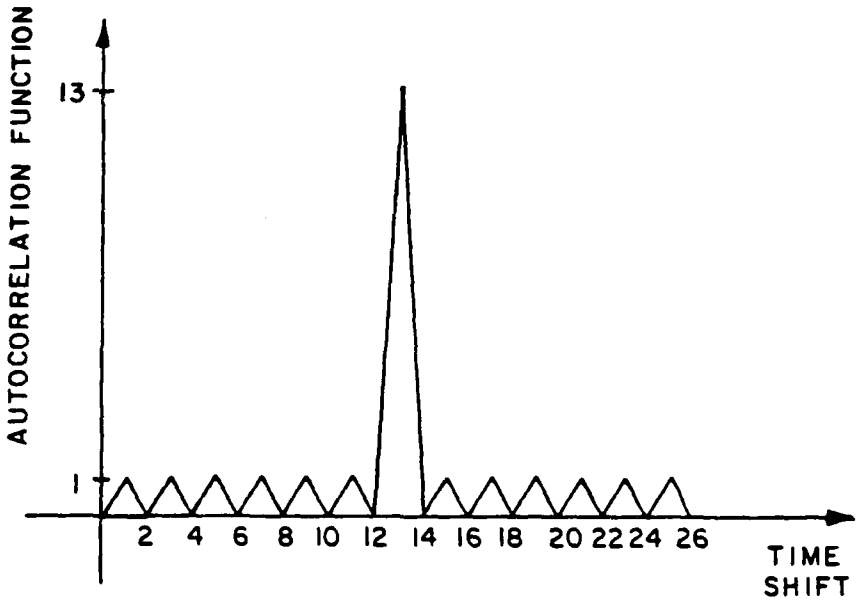

Figure 25: Autocorrelation Function of a 13-bit Barker Code

a sharp peak at zero shift and then drops to a constant value of $\frac{1}{N}$ for shifts over 1 bit, where N is number of bits in the code. Figure 26 shows the autocorrelation function of a PN code.

Figure 27 shows the signal processing at the array. At the array output is a filter matched to Code 1, followed by a threshold detector and a reference signal generation circuit. With the array in its uniform coverage mode, an arriving packet passes through the array and into the matched filter. The output of this filter, which is matched to Code 1 of the preamble, contains a sharp peak at the end of Code 1. This peak triggers the threshold detector and starts generation of a reference signal during Code 2. The reference signal is a signal identical to the received packet code during Code 2. The timing spike starts the reference signal at the proper time so it is highly correlated with the received packet during Code 2. The reference signal continues only during Code 2.

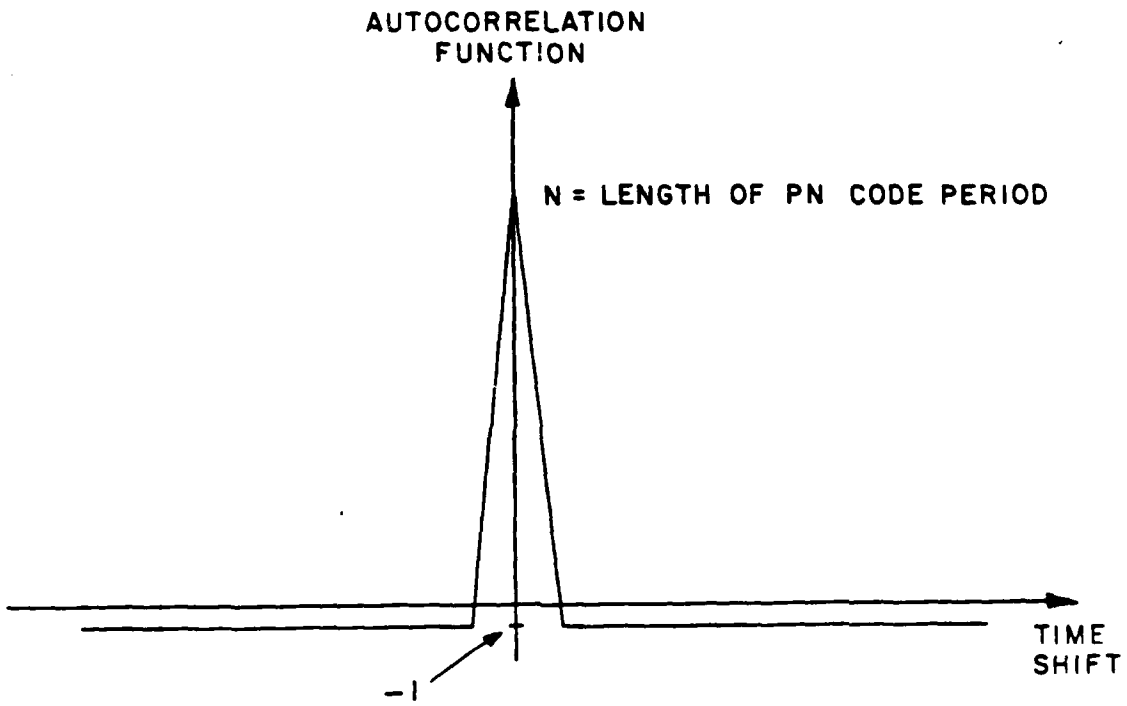

Figure 26: Autocorrelation function of a PN Code

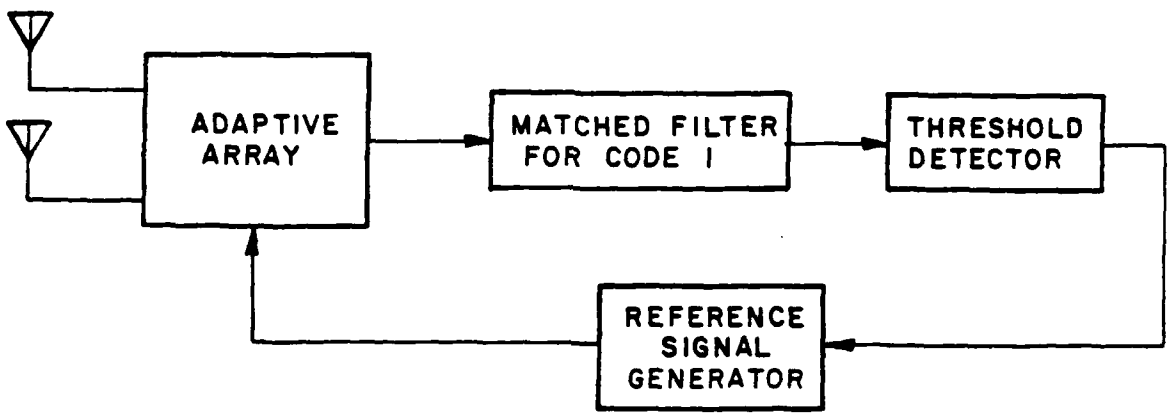

Figure 27: Packet Acquisition Circuitry

The reference signal is used in one of two ways, depending on whether the packet system is slotted or unslotted.

Acquisition in a Slotted System

For a slotted system, the following approach is used. The slot width, T_S, is made larger than the packet width, T_p, by an *uncertainty interval* T_U, as shown in Figure 28. The starting times of packet transmissions from all stations are randomized over the interval T_U. This uncertainty interval is included for two reasons. First, it makes the acquisition process fair by preventing stations closest to the repeater from always capturing the repeater first when two or more stations transmit. Second, it allows control over the probability that two packets arrive at the same instant. This probability has a significant effect on the packet throughput.

At the beginning of every slot, the array is put in its uniform coverage mode. Every user in the net then has equal access to the repeater. The first packet received in each slot initiates the lockup sequence and is normally the packet acquired by the array in that slot.

Suppose first that only one packet arrives during a slot. This packet causes a timing spike at the matched filter output. The timing spike switches the array into its adaptive mode and also triggers generation of a reference signal during Code 2. During Code 2, the adaptive array operates as an LMS array. The reference signal code is synchronized with Code 2 of the packet, and the array optimizes its weights for reception of the packet.[1] The response time of the array is chosen so the pattern has finished adapt-

[1]The reference signal does not have to be locked to the received packet in frequency or phase for this process to work. The only requirements are that the PN codes be synchronized to within about one quarter of a code bit, and that the difference between the reference signal frequency and the received signal frequency be less than the array feedback loop bandwidth [20],[21].

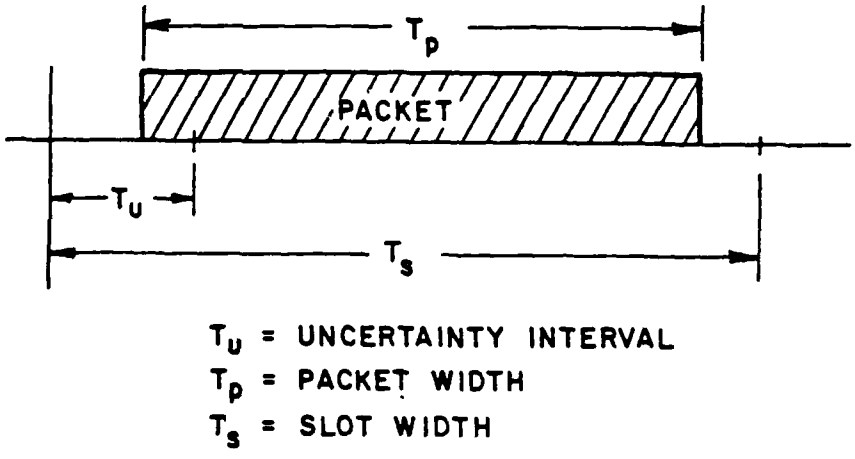

Figure 28: Slot Width, Packet Width, and Uncertainty Interval

ing during Code 2. At the end of Code 2, the array weights are frozen and the array pattern remains fixed during the address and message portions of the packet.

Now suppose two or more packets are received in the same slot. Each of these packets causes a timing spike at the matched filter output. However, only the first timing spike triggers reference signal generation and begins the array adaptation. The acquisition circuit is designed so that once it has been triggered, it does not repeat again in the same slot. Timing spikes after the first one in each slot are ignored.

Because the reference signal code is aligned with Code 2 of the first packet, it is uncorrelated with the second packet *as long as the second packet is at least one bit later than the first.* This is so because the autocorrelation function of a PN code has a very low value for shifts of 1 bit or more. (See Figure 26.) The second packet and all later packets are therefore treated

as interference by the adaptive array and are nulled. At the end of Code 2, the array pattern is optimized for reception of the first packet and has nulls on subsequent packets in the same slot.

If the second packet arrives *less than one bit after the first*, the array will probably not acquire the first packet properly. In this case there will be no throughput for that slot. With the uncertaintly interval T_U properly chosen, however, the probability of this event is small. Our analysis of channel throughput incorporates the probability of this event.

For this technique to work, it is necessary that the uncertainty interval T_U and the durations of Codes 1 and 2 be chosen so all packets in a given slot arrive before the end of the Code 2 segment in the first packet of the slot. However, it is not difficult to meet this condition. In our study we have shown that the uncertainty interval need not be longer than 100 bits, and Code 2 typically consists of one period of a 255 bit PN code. With this choice of parameters, every packet in a slot must start before the end of Code 2 for the first packet, because the uncertainty interval is shorter than Code 2. For this reason it is appropriate to operate with a fixed pattern during the address and message segment. The pattern obtained during Code 2 nulls all interfering packets and then the nulls are retained for the rest of the slot.

At the end of each slot, the array is again set into its uniform coverage mode, and the acquisition cycle starts over in the next slot.

Acquisition in an Unslotted System

In an unslotted system, packets can arrive at any time. In this case, the array must be able to adapt during the message portion of an acquired packet, in case a new interfering packet suddenly appears. Therefore a slightly different lockup technique is used.

For an unslotted system, the array is put in its uniform coverage mode whenever it is ready to receive a new packet. When a new packet arrives, it causes a timing spike at the matched filter output and triggers the reference signal generation, as in a slotted system. However, for an unslotted system, the array is left in its uniform coverage mode during Code 2. This interval is used *not* to adapt, but to derive a steering vector. The steering vector is obtained by multiplying the received signal on each array element by the reference signal and integrating the result over the duration of Code 2. The resulting vector is an estimate of the optimal steering vector for pointing a maximum gain pattern at the incoming packet. If interfering packets are present, this technique still yields a valid estimate of the required steering vector *as long as the second packet is at least one bit later than the first.* A delay of one bit or more decorrelates the interfering packet from the reference signal. If a second packet arrives *less than one bit after the first*, the estimated steering vector will be in error. In this case the first packet is not received correctly when this steering vector is used, so there is no throughput for that packet. The probability of this event is taken into account in our analysis.

For an unslotted system, the array operates as an Applebaum array using the estimated steering vector during the address and message segments. The array nulls any new packets that arrive during this interval. This procedure is appropriate for an unslotted system, because interfering packets can appear at any time.

In the unslotted system, an interfering packet arriving during the message part of a previously acquired packet causes a burst error in the received bit stream. Even though the adaptive array nulls the interfering packet, a finite amount of time is required to do so. During the adaptation transient,

the acquired packet suffers a burst error. To maintain throughput, it is therefore necessary in an unslotted system to use a burst error correction code.

Once the array is triggered by an incoming packet, the acquisition cycle continues until the end of that packet. At the end of the packet, the array is reset into its uniform coverage mode and is then ready to acquire the next packet.

These are the array acquisiton techniques we have considered for slotted and unslotted systems. For each case, we have done a theoretical analysis and simulations to determine the throughput and delay characteristics of a repeater using this technique.

Figure 29 shows a typical result. It shows the throughput S for a slotted channel using an adaptive array as a function of the traffic rate G. The throughput S is the average number of packets successfully received per packet length. (A throughput of unity is ideal and represents 100% use of the channel.) The traffic rate G is the average number of packets transmitted in the net per packet length. G includes both new packets and retransmissions of previously unsuccessful packets. The curves in Figure 29 are derived under the assumption of an infinite population of users transmitting packets with Poisson arrival times at an average rate of G packets per packet length. In Figure 29, the parameter N is the number of degrees of freedom available for nulling in the adaptive array [1]. The curves in Figure 29 have been computed for an uncertainty interval T_U of 100 bits and a 2° null resolution in the adaptive array.

The curve for $N = 0$ in Figure 29, which peaks at 36%, represents the classical slotted ALOHA result, when there is no adaptive array. Note that a modest adaptive array with 4 nulls, for example, can provide a

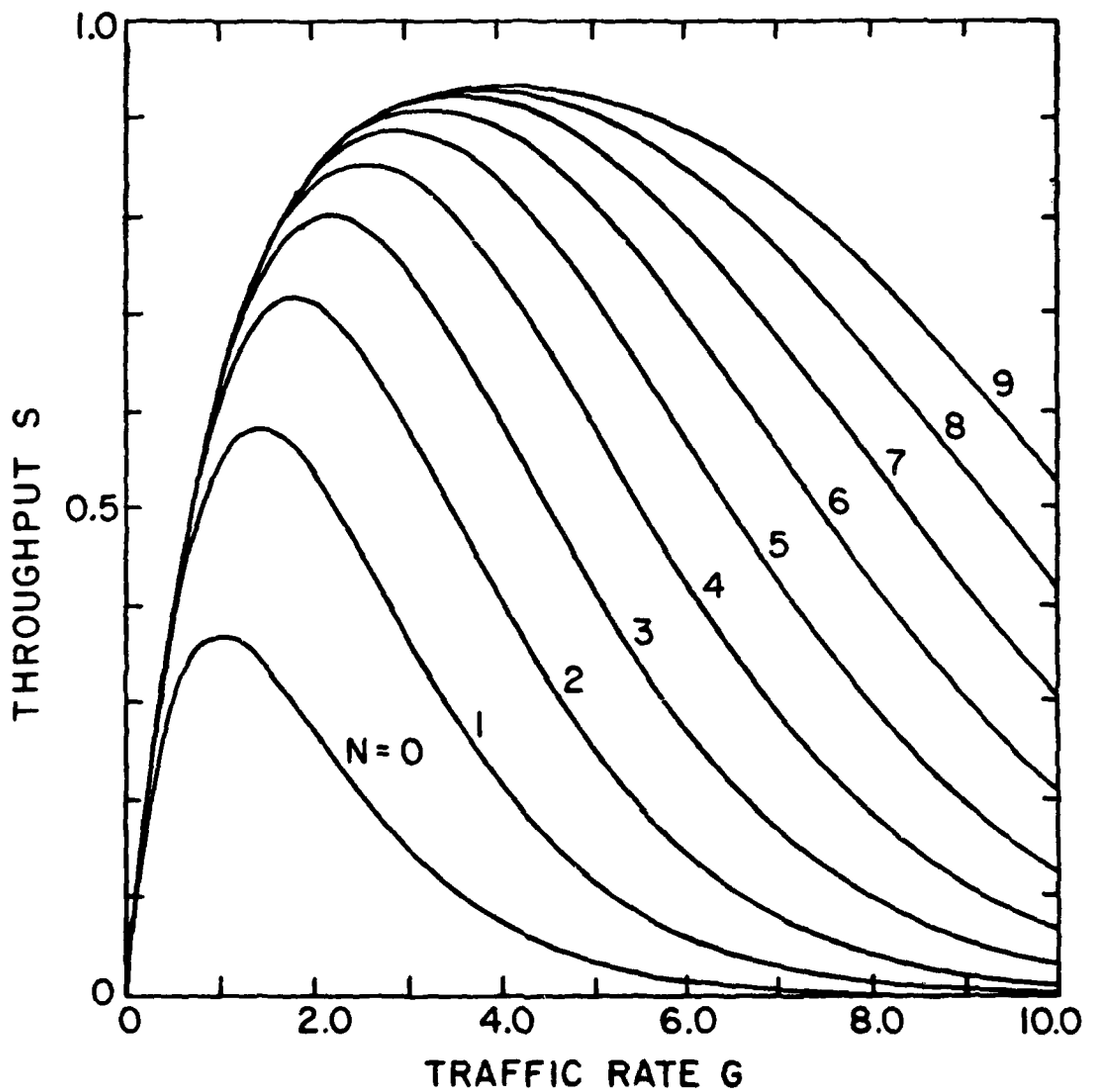

Figure 29: Throughput versus traffic rate with an adaptive array

peak throughput of 85%, a dramatic improvement over the 36% result for classical ALOHA.

Figure 29 shows typical performance improvements that are possible with an ordinary adaptive array in a packet radio system. However, it turns out that even more dramatic improvements are possible. Under JSEP we are studying what happens in a packet radio system if the adaptive array can form more than one pattern at the same time.

When an adaptive array is implemented in digital form, the signal on each element is brought to baseband and digitized in I and Q channels. The array beamforming is then done in software; the sampled element signals are multiplied by a set of weights and then added to produce the sampled array output. The pattern is adapted by changing the weights used.

However, in a digital adaptive array, it is possible to form more than one pattern at the same time from the same set of antenna elements. All that is required is to combine the element signals with more than one set of weights. If two sets of weights are used, for example, the two sets of weights can be controlled separately, and two independent array patterns will be produced.

At a packet radio repeater, one can use an adaptive array with multiple simultaneous beams to receive more than one packet at the same time. Two packets can be received in the same slot, for example, by providing two packet acquisiton loops of the type shown in Figure 27 at the array output. Each acquisition loop contains a matched filter, a threshold detector and a reference signal generator. One acquisition loop is used to lock the first array pattern on the first packet to appear in a slot. The second acquisition loop is disabled until after the first loop has locked. If a second packet arrives in the same slot, it is acquired by the second acquisition loop. The

first loop generates a set of array weights whose pattern tracks the first packet and nulls the second. The second loop generates a pattern that tracks the second packet and nulls the first. In this way, as long as the 2 packets do not start simultaneously, *both* packets are correctly received.

Figure 30 shows a typical throughput S achieved by such a system as a function of the traffic rate G. The parameter N is again the number of nulls available in each of the two patterns. (These curves are for an uncertainty interval of 100 bits and a null resolution width of 2°.)

Note that throughputs greater than unity are now possible! An array with only 2 nulls, for example, gives a peak throughput of about 1.15 packets per packet length.

A throughput greater than unity simply means that it is possible for the repeater to receive incoming packets at a faster rate than it can retransmit them on the downlink. A throughput greater than unity cannot be used unless the downlink is designed with higher capacity than the uplink. However, the potential of achieving throughputs greater than unity means that such a system could be operated at channel capacity and still have some margin available in the uplink.

5. Neural Nets

Under JSEP we have also done a small amount of research on memory storage in Hopfield neural networks [22],[23]. The purpose of this work was to determine how many stable pattern vectors can be stored in a Hopfield net. This work has resulted in one M.Sc. thesis [24].

Abu-Mostafa and St. Jacques [25] have derived a theoretical limit on the number of random patterns that can be stored in a Hopfield net. They show that the number of randomly generated patterns that can be stored

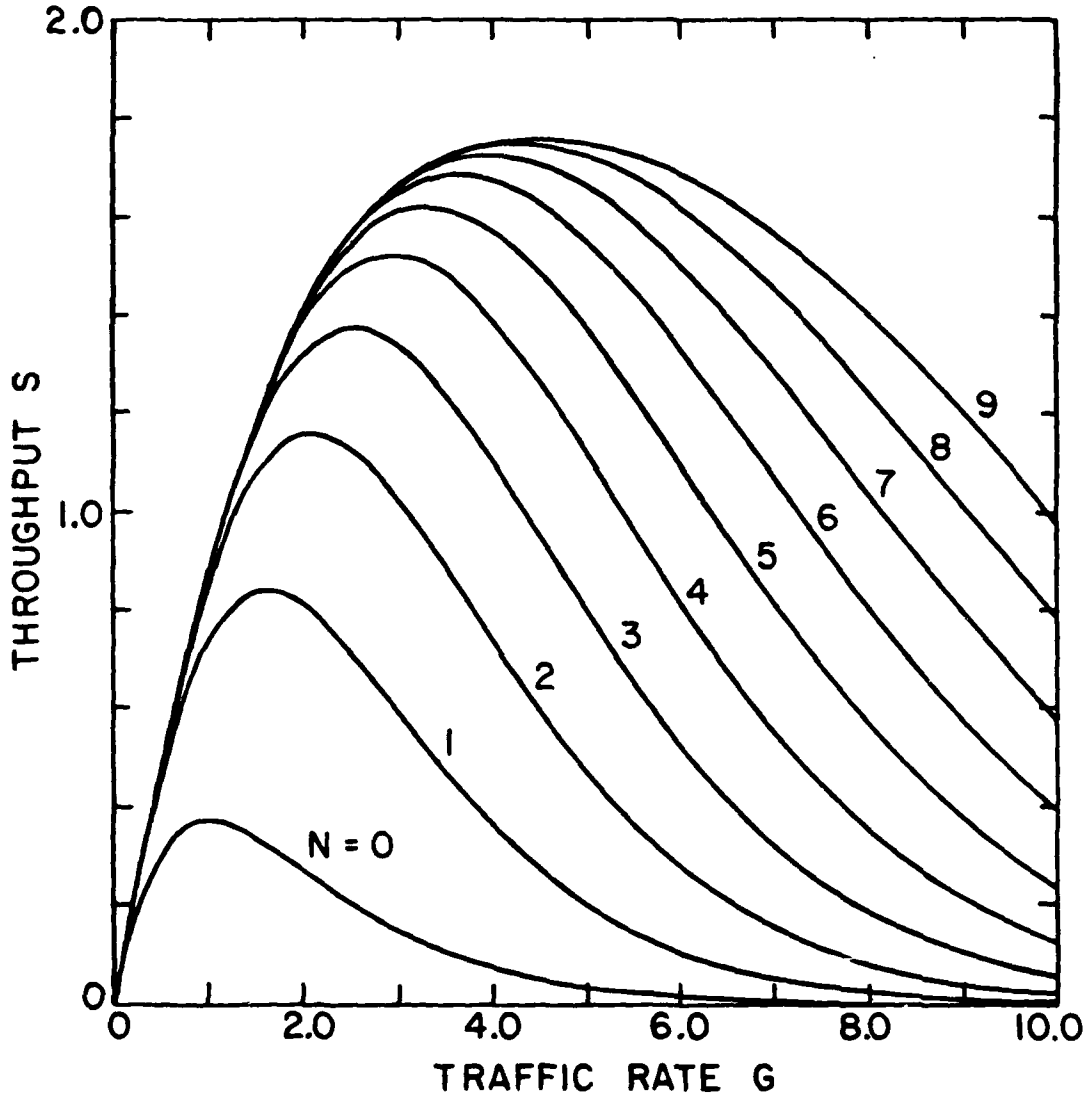

Figure 30: Throughput versus traffic rate with 2 simultaneous patterns

in an N-neuron Hopfield network is of the order of N regardless of the method used to store the information. This limited storage capacity is a result of the stringent requirement that any arbitrary set of K exemplars be able to be made stable. (Wallace obtained an algorithm for storing numbers of exemplars very near this limit [26]. His method provides for the storage of any set of N exemplars in a network of N neurons.) Our own work differed from that of Abu-Mostafa and St. Jacques [25] in that we did not attempt to store a randomly chosen set of states, but instead determined a specific set of states that can be stored. We found that a Hopfield network can store far more than the $0.15N$ states found by Hopfield, if these states are chosen in a certain way. Specifically, a network of N neurons with a transmission (synaptic gain) matrix T whose elements are all -1 except for the diagonal elements, which are all 0, can store up to $\frac{N!}{[(N/2)!]^2}$ stable vectors. The number of stable vectors for this transmission matrix grows exponentially with the number of neurons in the network. For a 100 node network, for example, Hopfield's algorithm for choosing the transmission coefficients produces about 15 stable vectors, and Wallace's training algorithm produces about 100 stable vectors. But the transmission matrix discussed above has about 10^{29} stable vectors, if the vectors are chosen properly. We also found a method for systematically reducing the number of stable states in enlarge the basis of attraction around each state [24].

6. References

[1] R.T. Compton, Jr., *Adaptive Antennas - Concepts and Performance*, Prentice-Hall, Inc., Englewood Cliffs, NJ, 1988.

[2] J.T. Mayhan, A.J. Simmons and W.C. Cummings, "Wideband Adaptive Antenna Nulling Using Tapped Delay-Lines," IEEE Transactions on Antennas and Propagation, AP-29, 6 (November 1981), 923.

[3] W.D. White, "Wideband Interference Cancellation in Adaptive Sidelobe Cancellers," IEEE Transactions on Aerospace and Electronic Systems, AES-19, 6 (November 1983), 915.

[4] R.T. Compton, Jr., "The Bandwidth Performance of a Two-Element Adaptive Array with Tapped Delay-Line Processing," IEEE Transactions on Antennas and Propagation, AP-36, 1 (January 1988), 5.

[5] R.T. Compton, Jr., "The Relationship between Tapped Delay-Line and FFT Processing in Adaptive Arrays," IEEE Transactions on Antennas and Propagation, AP-36, 1 (January 1988), 15.

[6] F.W. Vook and R.T. Compton, Jr., "The Bandwidth Performance of Multielement Adaptive Arrays with Tapped Delay-Line Processing," in preparation.

[7] Joint Services Electonics Program, Ninth Annual Report, Report No. 718109-1, December 1986, The Ohio State University ElectroScience Laboratory, Columbus, OH; prepared for Department of the Navy, Office of Naval Research under Contract N00014-78-C-0049.

[8] F.W. Vook, "The Bandwidth Performance of Multielement Adaptive Arrays with Tapped Delay-Line Processing," M. Sc. Thesis, Department of Electrical Engineering, Ohio State University; in preparation.

[9] M.W. Ganz, "Performance of Digital Communication Systems with Adaptive Arrays," Ph.D. Dissertation, August 1986, Department of Electrical Engineering, Ohio State University, Columbus, OH 43210.

[10] M.W. Ganz and R.T. Compton, Jr., "Protection of PSK Communication Systems with Adaptive Arrays," IEEE Transactions on Aerospace and Electronic Systems, AES-23, 4 (July 1987), 528.

[11] M.W. Ganz and R.T. Compton, Jr., "The Effects of Gaussian Interference on Communication Systems with Adaptive Arrays," IEEE Transactions on Aerospace and Electronic Systems, AES-23, 5 (September 1987), 654.

[12] M.W. Ganz and R.T. Compton, Jr., "Protection of a Narrow-Band BPSK Communication System with an Adaptive Array," IEEE Transactions on Communications, COM-35, 10 (October 1987), 1005.

[13] M.W. Ganz and R.T. Compton, Jr., "A Data-Derived Reference Signal Technique for Adaptive Arrays," to appear in IEEE Transactions on Communications.

[14] M.W. Ganz and R.T. Compton, Jr., "Protection of a BPSK Communication System with an Adaptive Array," MonTech Conference on Antennas and Communications, Sept.29-Oct.2, 1986, Montreal, Quebec, Canada.

[15] M.W. Ganz and R.T. Compton, Jr., "A Data-Derived Reference Signal Technique for Adaptive Arrays," 1987 IEEE AP-S International Symposium, June 15-19, 1987, Blacksburg, VA.

[16] L. Kleinrock and F.A. Tobagi, "Packet Switching in Radio Channels: Part I - Carrier Sense Multiple-Access Modes and Their Throughput-Delay Characteristics," IEEE Transactions on Communications, COM-23, 12 (December 1975), 1400.

[17] S. Lin and D.J. Costello, Jr., *Error Control Coding: Fundamentals and Applications*, Prentice-Hall, Inc., Englewood Cliffs, NJ, 1983.

[18] M.I. Skolnik, *Radar Handbook*, McGraw-Hill, Inc., New York, NY, 1970.

[19] S.W. Golomb, *Shift Register Sequences*, Holden-Day, Inc., San Francisco, CA, 1967.

[20] D.M. DiCarlo and R.T. Compton, Jr., "Reference Loop Phase Shift in Adaptive Arrays," IEEE Transactions on Aerospace and Electronic Systems, AES-14, 4 (July 1978), 599.

[21] D.M. DiCarlo, "Reference Loop Phase Shift in an N-Element Adaptive Array," IEEE Transactions on Aerospace and Electronic Systems, AES-15, 4 (July 1979), 576.

[22] J.J. Hopfield, "Neural Networks and Physical Systems with Emergent Collective Computational Abilities," Proc. Natl. Acad. Sci. USA, 79 (April 1982), 2554.

[23] D.W. Tank and J.J. Hopfield, "Collective Computation in Neuronlike Circuits," Scientific American, 257, 6 (December 1987), 625.

[24] M.N. Fulan, "A Hopfield Network with Exponential Storage Ability," M.Sc. Thesis, Department of Electrical Engineering, Ohio State University, Columbus, OH 43210.

[25] Y.S. Abu-Mostafa and J.M. St. Jacques, "Information Capacity of the Hopfield Model," IEEE Transactions on Information Theory, IT-31, 4 (July 1985), 461.

[26] D.J. Wallace, "Memory and Learning in a Class of Neural Network Models," in B. Bunk and K.H. Mutter (Eds.), *Proceedings of the Workshop on Lattice Gauge Theory*, Wuppertal, 1985, 313.

7. List of Papers - JSEP Hybrid Studies

Published:

1. M.W. Ganz, R.T. Compton, Jr., "The Effects of Gaussian Interference on Communication Systems with Adaptive Arrays," *IEEE Transactions on Aerospace and Electronic Systems*, Vol. AES-23, No. 5, pp. 654- 663, September 1987.

2. A.S. Al-Ruwais, R.T. Compton, Jr., "Adaptive Array Behavior with Periodic Phase Modulated Interference," *IEEE Transactions on Aerospace and Electronic Systems*, Vol. AES-23, No. 5, pp. 602-611, September 1987.

3. M.W. Ganz, R.T. Compton, "Protection of a Narrow-Band BPSK Communication System with an Adaptive Array," *IEEE Transactions on Communications*, Vol., COM-35, No. 10, pp. 1005-1011, October 1987.

4. R.T. Compton, Jr., "The Bandwidth Performance of a Two-element Adaptive Array with Tapped Delay-Line Processing," *IEEE Transactions on Antennas and Propagation*, Vol. AP-36, No. 1, pp. 5- 14, January 1988.

5. R.T. Compton, "The Relationship Between Tapped Delay-Line and FTT Processing in Adaptive Arrays," *IEEE Transactions on Antennas and Propagation*, Vol. AP-36, No. 1, pp. 15-26, January 1988.